Am J Transl Res 2017;9(6):3120-3137
www.ajtr.org /ISSN:1943-8141/AJTR0050914

Original Article

MicroRNA-1825 induces proliferation of adult cardiomyocytes and promotes cardiac regeneration post ischemic injury

Raghav Pandey[1], Sebastian Velasquez[1], Shazia Durrani[1], Min Jiang[2], Michelle Neiman[4], Jeffrey S Crocker[1], Joshua B Benoit[3], Jack Rubinstein[2], Arghya Paul[5], Rafeeq PH Ahmed[1]

[1]Department of Pathology and Laboratory Medicine, [2]Department of Internal Medicine, Division of Cardiovascular Diseases, [4]Department of Molecular and Cellular Physiology, College of Medicine, University of Cincinnati, Cincinnati 45267, OH, USA; [3]Department of Biological Sciences, University of Cincinnati, Cincinnati 45220, OH, USA; [5]Department of Chemical and Petroleum Engineering, School of Engineering, University of Kansas, Lawrence 66045, KS, USA

Received February 15, 2017; Accepted May 9, 2017; Epub June 15, 2017; Published June 30, 2017

Abstract: In mammals, proliferative capacity of cardiomyocytes is lost soon after birth, while zebrafish and other lower organisms like newts are known to regenerate injured hearts even at an adult age. Here, we show that miR-1825 can induce robust proliferation of adult rat cardiomyocytes and can improve cardiac function in-vivo post myocardial infarction. Rat adult cardiomyocytes transfected with miR-1825 showed a significant increase in DNA synthesis, mitosis, cytokinesis, and an increase in cell number when compared to cel-miR-67 transfected control. We also observed a reduction in mitochondrial number and a decrease in ROS and DNA-damage. RNA-sequencing data identified NDUFA10, a key gene involved in the mitochondrial electron transport chain to be a direct target of miR-1825. SiRNA mediated silencing of NDUFA10 showed a significant increase in cardiomyocyte proliferation indicating its role downstream of miRNA-1825. In addition, microRNA microarray results identified miR-1825 to regulate expression of a known proliferation inducing miRNA, miR-199a. We also identified the direct targets of miR-199a, namely p16, Rb1, and Meis2 to be downregulated following miR-1825 transfection. However, miR-199a alone did not have similar proliferation inducing effects as miR-1825, indicating that miR-1825 works through multiple pathways and is a master regulator of cardiomyocyte proliferation. In addition, our *in-vivo* analysis in animal models of LAD ligation and intra-cardiac miRNA delivery showed proliferation of endogenous cardiomyocytes in the peri-infarcted region and an improvement in heart function. These findings establish miR-1825 as a potential therapeutic agent for induction of cardiomyocyte proliferation and cardiac regeneration, with a significant translational potential.

Keywords: MicroRNA, adult cardiomyocytes, proliferation, hydrogel, cardiac regeneration, mitochondrial biogenesis

Introduction

Cardiovascular disease claims over 17 million lives each year worldwide and for decades has been the biggest killer in the United States [1-4]. The major factor contributing to this is the terminally differentiated nature of the adult mammalian heart and the inability of cardiomyocytes to proliferate [5-7]. While there are reports about limited turnover of cardiomyocytes in an adult heart, it is still insufficient to replenish the loss of cardiomyocytes following a myocardial injury [8]. However, in lower amphibians like zebrafish, a robust resuscitation of cardiac tissue is observed following injury [8, 9]. A molecular understanding of this phenomenon has been extensively researched, leading to exogenous delivery of genes, miRNAs, and small molecules to induce proliferation and differentiation of mammalian cardiomyocytes by promoting cell cycle re-entry of both mice and rat cardiomyocytes [9].

Recent studies have shown that the reduction in proliferative capacity during the post neonatal stage in mammalian hearts is due to the increase in tissue oxygen content. Increase in oxygen concentration has also been shown to

increase mitochondrial mediated oxidative phosphorylation, leading to higher levels of reactive oxygen species (ROS) production, subsequent DNA damage and activation of DNA damage response (DDR) pathways [10, 11], eventually leading to cell cycle arrest. Supporting this hypothesis, subsequent studies have reported that the majority of naturally proliferating cardiomyocytes in an adult heart (~1% annually) have an affinity for a hypoxic niche [10].

The discovery of miRNAs by Ambros and colleagues in the early 1990s changed the worldview of these small RNA strands, which are found to regulate a plethora of biological processes [12-15]. Breakthroughs in the field of cardiovascular research came around the late 2000s, when the first cardiac miRNAs associated with cardiac remodeling were discovered. In less than a decade, there were studies proposing miRNAs as therapeutics for cardiac diseases [16]. While the importance of miRNA in regulating biological pathways and their mode of action involving binding to the 3'UTR and silencing target genes is well established, there have been very few reports on miRNA regulating other miRNAs [17-21]. Here we report one such master regulator miRNA, miR-1825. We show that miR-1825 acts as a master regulator regulating miR-199a (also reported to be involved in proliferation induction in neonatal and adult cardiomyocytes [9]). Together, miR-1825 reduces mitochondrial mass and function by directly inhibiting NDUFA10 (mitochondrial membrane protein involved in electron transport chain), inhibits cell-cycle genes (Retinoblastoma1 [Rb1] and Meis2, through miR-199a), and induces robust proliferation of adult cardiomyocytes. In addition miR-1825 also reduces oxidative stress and protects against reactive oxygen species (ROS) mediated DNA damage and DNA damage response (DDR) pathway. Moreover, sustained delivery of miR-1825 promoted cardiomyocyte proliferation, induced regeneration of ischemic myocardium post LAD ligation, reduced infarction size, and improved heart function (echocardiography).

Methods

Ethical statement

All protocols were approved by the Institutional Animal Care and Use Committee of the University of Cincinnati, College of Medicine (IACUC). All experiments performed followed the guidelines of the Guide for the Care and Use of Laboratory Animals published by the US National Institutes of Health (NIH).

Isolation of adult rat ventricular cardiomyocytes

Ventricular cardiomyocytes were isolated from 8-12 weeks old male rat hearts using the Langendroff-perfusion method as described earlier [22]. See Supplementary Methods for detailed protocol. Animals were euthanized with an overdose of sodium pentobarbital.

Transfection

Adult rat cardiomyocytes were transfected (24 hours post plating) with 50 nM miRNA mimics (Dharmacon, GE) using lipofectamineRNAiMAX (Life Technologies) using a standard transfection protocol (Life Technologies). Briefly, miRNA mimic and lipofectamine were diluted separately in OPTI-MEM (Life Technologies). The two were mixed together for 15 min and added to cardiomyocytes in antibiotic free DMEM medium.

Immuno-staining

Cells were fixed with 4% paraformaldehyde for 15 min and permeabilized with 0.5% Triton X-100 in PBS for 20 minutes. Cells were then stained with specific primary antibodies and respective conjugated secondary antibodies (in CAS-Block, Life Technologies) overnight at 4°C. See Supplementary Methods for detailed protocol and antibodies used.

Image analysis

Following staining, TMRM, VDAC, dihydrorhodamine 123, and CellRox levels were measured using ImageJ software, where each image was taken at the same intensity and pixels per area were quantified across 30 cells per condition per trial ($n \geq 3$ trials).

Western blot

Wes Protein Simple (Protein Simple, CA) a newer technique that is getting widely accepted, was used to perform western blot protein analysis of cardiomyocytes transfected with miRNA mimics [23, 24]. Total protein was isolated using standard protocols, using RIPA buf-

fer with protease/phosphatase inhibitors (Roche). Using manufacturer's instructions, premade plates were loaded with protein samples, primary and secondary antibodies (manufacturer provided) and were run on Wes ProteinSimple as per manufacturer's instructions. Protein bands were analyzed using Image-J (NIH) software. Traditional Western-blots were performed for some proteins (specified in the figure legend), by separating proteins on a 4-12% sodium dodecyl sulfate-polyacrylamide gels (Invitrogen), transferred to a PVDF membrane, and blocked with 5% non-fat milk (Bio-Rad), followed by labelling with primary antibodies and horseradish peroxidase conjugated secondary antibodies. See Supplementary Methods for detailed protocol and antibodies used.

RNA-sequencing analysis

Adult cardiomyocytes transfected with cel-miR-67 or hsa-miR-1825 were used to isolate total RNA using Trizol (Invitrogen) and according to the manufacturer's protocol using mirVana-miRNA isolation kit (Invitrogen). Data was generated at the DNA sequencing and genotyping core located at Cincinnati Children's Hospital Medical Center, Cincinnati OH. See Supplementary Methods for detailed protocol.

Luciferase assay

293T cells were transfected with the luciferase construct containing 3'UTR of the genes of interest, according to the manufacturer's protocol (GeneCopoeia). MiR-1825 was transfected simultaneously (as described above) and media was harvested 48 hours post transfection and chemiluminuscence was measured using Glomax multi-detection system (Promega). See Supplementary Methods for 3'UTR sequence and binding site details.

Cardiomyocyte cell size

Neonatal mice heart sections on slides were stained with WGA (see Supplementary Methods) and cell area was quantified using ImageJ software (National Institute of Health) by tracing the boundaries of individual cells.

Myocardial infarction (permanent occlusion) of adult mice hearts

All protocols were approved by the Institutional Animal Care and Use Committee of the University of Cincinnati, College of Medicine (IACUC). AAV9 virus was used for transduction in-vivo. To determine the role of miR-1825 on regenerating ischemic myocardium, 22-week old, female, C57BL/6 mice were used for the study (n = 9 for AAV-GFP control and n = 10 for AAV-miR-1825). Surgeries were performed on sedated mice (isofurane, Abbott Laboratories). Left Anterior Descending Artery (LAD) was ligated (permanent occlusion) and successful infarction was confirmed using electrocardiogram (ECG). Mice were kept under constant anesthesia (Isoflurane) throughout the surgery. Buprenex (0.1 mg kg^{-1}) twice a day, was injected subcutaneously for pain relief.

Delivery of miR-1825 post MI in adult mice hearts and EdU administration

Following LAD ligation, the peri-infarcted region was transduced with 1×10^{11} viral particles of either AAV-GFP (n = 9) (control) and AAV-GFP-miR-1825 (n = 10), using an insulin syringe at two different locations. EdU (350 μg) was injected intraperitoneally, every other day, until day 12 post surgery.

Gel mediated delivery of miR-1825 post MI in adult mice heart and EdU administration

A biocompatible injectable gel consisting of gelatin and silicate was used to deliver the viral particles. This gel and its derivatives have been used in our earlier work for diverse biomedical applications [25-28]. The gel was used mainly to help protect the viral particles from immediate wash out by the beating heart and induce a sustained release of the particles from the gel for enhanced therapeutic outcome. In particular, 5% gelatin (Sigma-Aldrich, St Louis MO), 2% silicate was dissolved in ddH_2O and maintained at 37°C till the time of injection.

Following LAD ligation, the peri-infarcted region was transduced with 2×10^9 viral particles (AAV-miR-1825 or AAV-GFP) together with hydrogel in total 20 uL volume (10 uL Gel + 10 uL viral particles), at two different locations. EdU (350 μg) was injected intraperitoneally, every other day, until day 12 post surgery.

Echocardiography

Heart function was evaluated by transthoracic echocardiography performance on sedated mice (isofurane, Abbott Laboratories) at 7, 14,

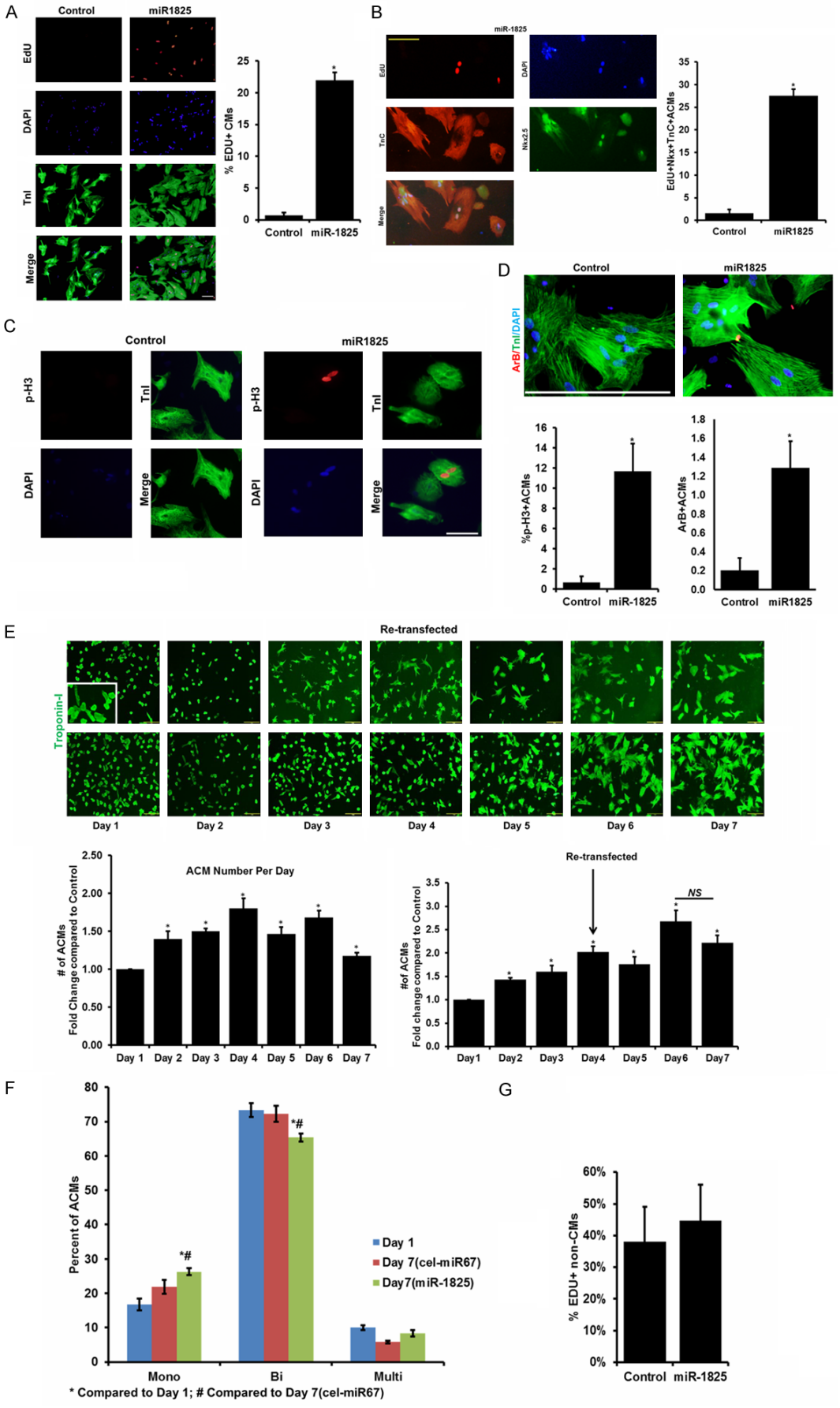
A
Control
miR1825
EdU
DAPI
TnI
Merge
% EDU+ CMs
Control
miR-1825
B
miR-1825
EdU
DAPI
TnC
Nkx2.5
Merge
EdU+Nkx+TnC+ACMs
Control
miR1825
C
Control
miR1825
p-H3
TnI
DAPI
Merge
D
Control
miR1825
ArB/TnI/DAPI
%p-H3+ACMs
ArB+ACMs
Control
miR-1825
E
Re-transfected
Troponin-I
Day 1
Day 2
Day 3
Day 4
Day 5
Day 6
Day 7
ACM Number Per Day
# of ACMs
Fold Change compared to Control
Re-transfected
#of ACMs
Fold change compared to Control
NS
F
Percent of ACMs
Day 1
Day 7(cel-miR67)
Day7(miR-1825)
Mono
Bi
Multi
* Compared to Day 1; # Compared to Day 7(cel-miR67)
G
% EDU+ non-CMs
Control
miR-1825

Figure 1. miR-1825 induces proliferation of naturally quiescent adult cardiomyocytes. (A) Adult cardiomyocytes (ACMs) transfected with either control miRNA (cel-miR-67) or miR-1825 mimic were immuno-stained for markers of DNA synthesis (EdU). (B) $EdU^+Nkx2.5^+TnC^+$ Cells to mark DNA synthesis in cardiac specific nuclei. (C) Mitosis (p-H3); (D) Cytokinesis (Aurora-B). (E) Adult CMs were counted each day either with single transfection on day 1 or double transfection on day 1 and day 4 (miR-1825 number compared to control). (F) Nuclear count in CMs; (G) DNA synthesis (EdU) in non-CMs. N≥3; *P<0.05. Troponin-I (TnI) used as cardiac cell marker; DAPI-nucleus. Scale bar = 200 μm (A, E), 100 μm (B).

and 28 days post-surgery. Briefly, mice were anesthetized with isoflurane and placed on the heated stage of the Vevo 2100. Parasternal long axis (PSLAX) and short axis (SAX) images were recorded and then analyzed on a separate work station with VevoStrain software (Vevo 2100, v1.6, Visualsonic, Toronto, Canada). For end-point studies on isolated hearts, animals were euthanized with overdose of sodium pentobarbital.

Statistics

Sample size in each experiment was ≥3; One and two-tailed student's t-test was used for statistical analysis and significance calculation. P<0.05 was used as the statistically significant difference. All quantifications and cell counting were blinded and counted by at least two individuals.

ANOVA One Way Analysis of Variance was performed for in-vivo experiments. *P<0.05 was considered significant.

Results

MiR-1825 induces robust proliferation of quiescent adult cardiomyocytes

Adult cardiomyocyte transfection efficiency was determined using fluorescent labelled Dy547-cel-miR-67 and siRNA mediated inhibition of Ubiquitin-C (siUbC) (>80% transfection efficiency; Supplementary Figure 1). These cells maintained their cardiac nature, evident by the regular beating observed on day 7 post-plating (Supplementary Video 1). Adult cardiomyocytes transfected with miR-1825 showed 21.99% of cells positive for EdU while control (cel-miR-67) had 0.71% of cells positive for EdU indicating a significant increase in DNA synthesis (**Figure 1A**). To confirm that only cardiomyocyte nuclei were counted we added a cardiomyocyte nuclear marker Nkx2.5 and counted $EdU^+TnC^+Nkx2.5^+DAPI^+$ cells and found over 25% EdU positive cardiomyocytes (**Figure 1B**). In addition 11.67% of cardiomyocytes transfected with miR-1825 were positive for mitosis, as shown by phospho-Histone H3 (ser-10) (**Figure 1C**) and 1.3% Aurora-B positive adult cardiomyocytes indicating cytokinesis (**Figure 1D**). Live cell imaging over a period of 20 hours (between day 3 and day 4, post transfection) showed real-time proliferation of adult cardiomyocytes in miR-1825 transfected group (Supplementary Video 2). Tracking cells each day also showed replication of single cardiomyocyte into two cells (Supplementary Figure 2). Cultured adult cardiomyocytes have been known to undergo de-differentiation evident from a decrease in Myh6, increase in Myh7, and an increase in Nkx2.5. We found a decrease in Myh6 and an increase in Nkx2.5 in cultured (d7) adult cardiomyocytes as reported earlier [9] (Supplementary Figure 3). Even though de-differentiation is seen in both the control and miR-1825 transfected groups, proliferation as shown by cell-cycle regulators like P16 and CyclinD1 (Supplementary Figure 4), was only seen in miR-1825 group. Moreover, this proliferative effect of miR-1825 was specific to cardiomyocytes and was not observed in cardiac fibroblast (**Figure 1G**). Next, we quantified the number of cells (counting cells each day) and found a 1.8 fold increase in cell number at day 4 post-transfection compared to control; however cell numbers declined on subsequent days which may be due to transient expression of miR-1825. To overcome this we re-transfected the cells on day 4 and observed a 2.5 fold increase in number of cells on day 6 (**Figure 1E**). Atrial natriuretic peptide (ANP), a marker for hypertrophy, showed fewer hypertrophied cardiomyocytes with miR-1825 (Supplementary Figure 5) when compared to control. Additionally, we found that cardiomyocytes transfected with miR-1825 showed significantly higher mono-nucleated cells, while bi-nucleated cell number was significantly lower when compared to both cardiomyocytes in culture for 1 day and control transfected cardiomyocytes (**Figure 1F**). This confirms that the increase in

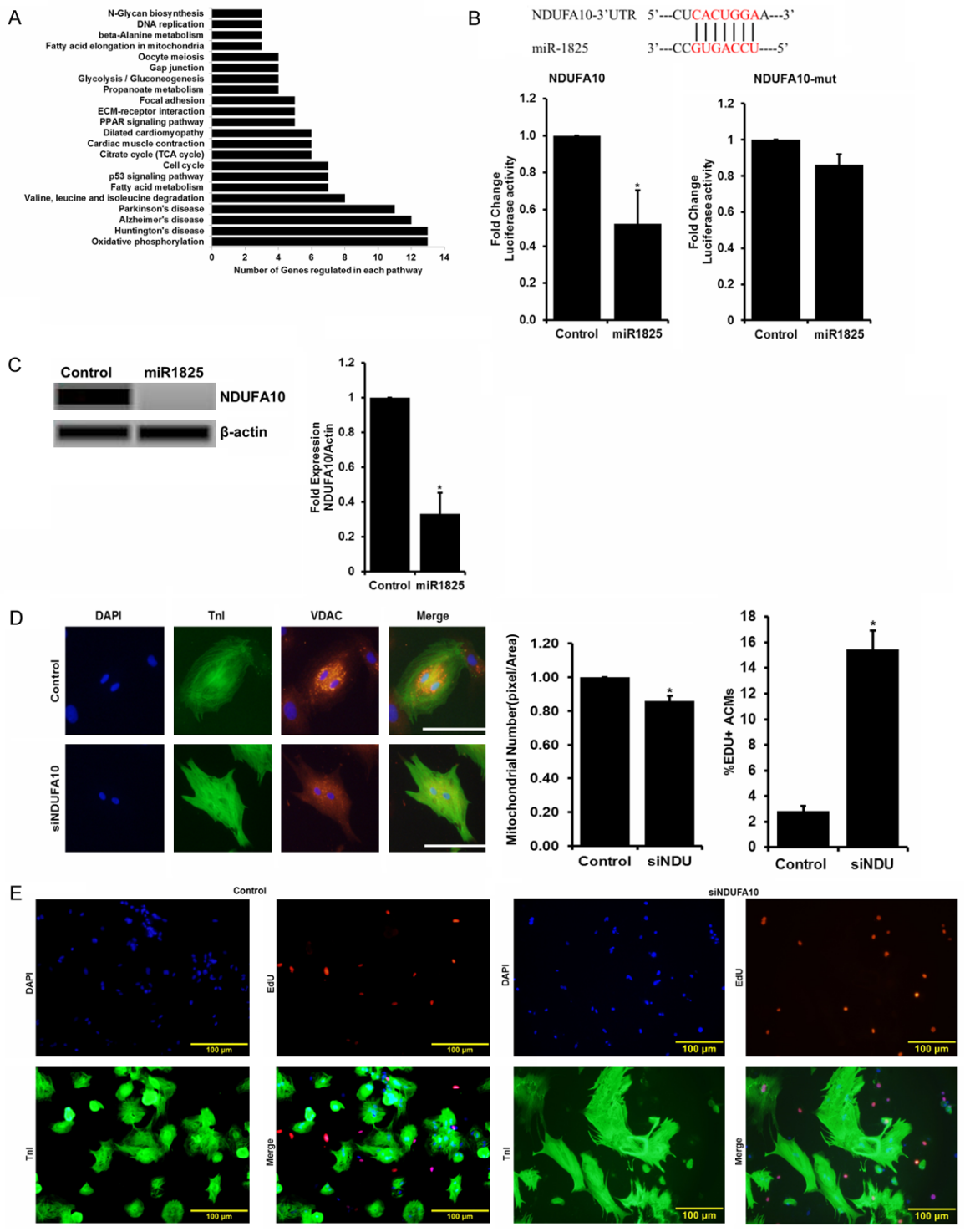

Figure 2. Mitochondria related genes are regulated by miR-1825. (A) Pathways altered in Adult cardiomyocytes (ACMs) transfected with miR-1825 compared to control ACMs revealed through RNA-sequencing analysis. (B) In-silico analysis indicating a direct binding site for miR-1825 on the 3'UTR of NDUFA10, confirmed with luciferase assay. (C) Protein level expression of NDUFA10 in Adult CMs transfected with miR-1825. (D) Mitochondrial number; (E) DNA synthesis post NDUFA10 gene knock-down in Adult CMs. N≥3; *P<0.05. VDAC used as mitochondrial marker; TnI used as cardiac cell marker; DAPI-nucleus. SiNDU = siNDUFA10. Scale bar = 100 μm (D), Scale bar = 100 μm (E). Control (cel-miR-67).

cardiomyocytes was a result of newly derived mono-nucleated cells. To detect if miR-1825 can also induce proliferation in human cardiomyocytes we transfected human induced pluripotent stem cell-derived (HiPS) cardiomyocytes (HiPS-CMs) with miR-1825 or cel-miR-67 (control) and our results reveal a very high rate of proliferation, with over 47.64% EdU^+ and 27.98% phospho-Histone H3 (ser-10) positive HiPS-CMs in miR-1825 group. (Supplementary Figure 6).

Genes related to mitochondrial function are regulated by miR-1825

A whole-transcriptome miRNA-microarray and RNA-sequencing in adult cardiomyocytes transfected with cel-miR-67 (control) and miR-1825 was performed (Genomics Core, CCHMC) and results (Supplementary Figure 7; NCBI Bioproject Accession number PRJNA308945) were analyzed using bioinformatics software and tools (CLC Genomics Workbench 5). Expression was based on transcripts per million (TPM) with significance determined by a Baggerly's test with the false detection rate of 0.05. Our RNA sequencing results identified over 300 genes regulated by miR-1825, involving several pathways including proliferation, cell cycle, apoptosis, oxidative phosphorylation, TCA cycle, and DNA-damage (**Figure 2A**). In addition to genes, several miRNAs were also regulated including miR-199a which has been previously reported to induce proliferation in neonatal cardiomyocytes [9]. The majority of genes downregulated by miRNA-1825 were involved in mitochondrial mediated oxidative phosphorylation (**Figure 2A**). Our RNA sequencing results identified down regulation of NADH Dehydrogenase (Ubiquinone) 1 Alpha Subcomplex, 10, 42 kDa (NDUFA10) and in-silico analysis identified a binding site in the 3'UTR of NDUFA10 for miR-1825, which was conserved in mice, rats, and humans. Luciferase assay using 3'UTR of NDUFA10 showed inhibition with miR-1825, as measured through luciferase activity, compared to cel-miR-67. However, this inhibition was not observed with mutated NDUFA10 3'UTR having deleted binding site for miR-1825 (**Figure 2B**). Protein levels of NDUFA10 were also significantly reduced in cardiomyocytes transfected with miR-1825, compared to control cells (**Figure 2C**). NDUFA10 is known to be involved in transport of electrons in the mitochondria and is located in the inner mitochondrial membrane [29]. Interestingly, siRNA mediated knockdown of NDUFA10 resulted in a significant decrease in the number of mitochondria (measured through mitochondrial wall membrane bound *voltage-dependent anion channel* [VDAC]) (**Figure 2D**), and a significant increase in EdU^+ adult cardiomyocytes (**Figure 2E**). We also confirmed the expression of other mitochondria related genes and interestingly, inhibition of NDUFA10 resulted in inhibition of COX in addition to NDUFA10, both at RNA and protein level (Supplementary Figure 8). Altogether, we confirmed that miR-1825 inhibits NDUFA10 and increases DNA synthesis (as shown through EdU^+ ACMs). Next, we determined the effects ofmiR-1825 on mitochondrial number and function, in addition to cell toxicity, DNA damage, and DNA damage response (DDR) which can result in cell cycle arrest.

MiR-1825 reduces mitochondrial mass, prevents ros production and inhibits DNA damage

To determine if regulation of NDUFA10 had an effect on mitochondrial mass we looked at VDAC, which is a mitochondrial outer membrane protein [30]. We identified VDAC expression levels to be significantly reduced in adult cardiomyocytes transfected with miR-1825 [and also with siNDUFA10 (**Figure 2D**)] when compared to the control group (**Figure 3A**) indicating fewer mitochondria. Moreover, transmission electron microscopy (TEM) revealed a significant reduction in mitochondria in miR-1825 transfected adult cardiomyocytes (**Figure 3B**). Next, we measured the mitochondrial mass using Cytochrome c oxidase (COX IV), which is a key enzyme that controls mitochondrial electron transport chain and frequently used as a measure of mitochondrial content [31]. A significant reduction is protein expression of COX-IV was observed in adult cardiomyocytes transfected with miR-1825 (Supplementary Figure 9). Moreover, ROS levels were also observed to be significantly lower with miR-1825 (**Figure 3C**) as shown by DiH123 immunostaining. Subsequently DNA damage response (DDR) activation was significantly hindered with miR-1825 (**Figure 3E**) as shown by reduced oxidized guanine (8Oxo-G) levels. In addition, miR-1825 had a protective role against H_2O_2 induced oxidative stress, as shown by reduced CellRox levels following treatment with 10 μM H_2O_2 (**Figure 3D**).

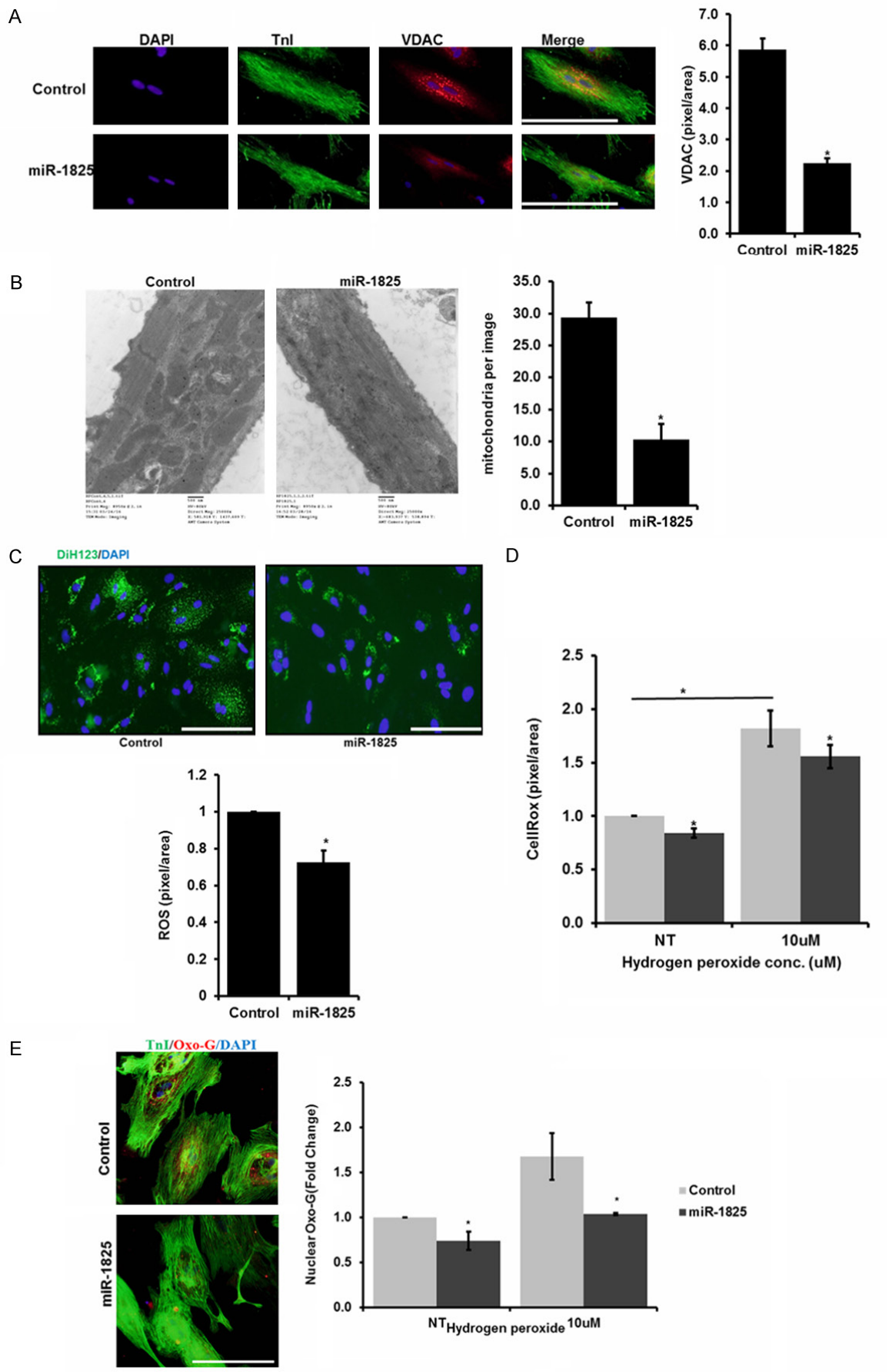
A
DAPI
TnI
VDAC
Merge
Control
miR-1825
VDAC (pixel/area)
7.0
6.0
5.0
4.0
3.0
2.0
1.0
0.0
Control
miR-1825
B
Control
miR-1825
mitochondria per image
35.0
30.0
25.0
20.0
15.0
10.0
5.0
0.0
Control
miR-1825
C
DiH123/DAPI
Control
miR-1825
ROS (pixel/area)
1.2
1
0.8
0.6
0.4
0.2
0
Control
miR-1825
D
CellRox (pixel/area)
2.5
2.0
1.5
1.0
0.5
0.0
NT
10uM
Hydrogen peroxide conc. (uM)
E
TnI/Oxo-G/DAPI
Control
miR-1825
Nuclear Oxo-G(Fold Change)
2.5
2.0
1.5
1.0
0.5
0.0
Control
miR-1825
NT
Hydrogen peroxide
10uM

Figure 3. miR-1825 reduces mitochondrial number and prevents ROS production and DNA damage. A. VDAC staining for mitochondrial number, bar graph represents quantification of VDAC expression by densitometry B. TEM images to visualize mitochondria in cardiomyocytes, bar graph represents number of mitochondria per image. C. ROS levels measured using DiH123, bar graph represents quantification of ROS expression by densitometry. D. Oxidative stress measured using Cell-Rox with NT (no treatment) or 10 μM H_2O_2 treatment. E. DNA-damage measured using nuclear 8-oxoG; bar graph represents quantification of nuclear 8-oxoG positive ACMs with NT or 10 μM H_2O_2 treatment in both the groups. N≥3; *P<0.05. Troponin-I used as cardiac cell marker; DAPI-nucleus. Scale bar = 200 μm. Control (cel-miR-67).

Master regulator, mir-1825 regulates proliferation inducing miRNA and genes

As determined by our RNA-sequencing data and confirmed by our qRT-PCR (**Figure 4A**), miR-199a was significantly increased in adult cardiomyocytes post miR-1825 transfection, indicating miR-199a to be downstream of miR-1825. Next, in-silico analysis determined that miR-199a has direct binding sites on the 3'UTR of cell cycle inhibitory genes Meis2 and Rb1. We confirmed the binding of miR-199a on the 3'UTR of Meis2 and Rb1, through luciferase assay and found a significantly decreased luciferase activity with miR-199a as compared to the control (**Figure 4B**). To delineate the percent contribution of miR-199a in the miR-1825 mediated increase in proliferation, we used different combinations of mimics and inhibitors. We observed that miR-199a induces a significant increase in proliferation when compared to control. Moreover, simultaneous delivery of miR-1825 and miR-199a inhibitors showed a significant decrease in proliferation, when compared to miR-1825 (Supplementary Figure 10). Moreover, while inhibition of neither of the miR-199a targets conferred a significant increase in proliferation, a simultaneous inhibition of Rb1 and Meis2 induced a significantly higher proliferation as seen through DNA synthesis marker EdU (**Figure 4C**). A similar trend was seen at the mitotic level in the adult cardiomyocytes with the combinations (**Figure 4D**). Altogether, this confirmed that miR-1825 mediated proliferation works partly through miR-199a and through its other downstream targets. We also confirmed an inhibition in protein level expression of Meis2 and Rb1 in cardiomyocytes transfected with miR-1825 (Supplementary Figure 10).

MiR-1825 mediated proliferation results in increased heart size and cardiomyocyte number in neonatal mice

Even though there are conflicting reports on the regenerative potential of neonatal hearts [32], it is widely accepted that the mammalian cardiomyocytes retain the ability to proliferate up until day 5 or 7 after birth, depending on the species, followed by a senescent state [33]. To determine if miR-1825 can extend this proliferative window, we injected one day old mice (n = 8) with either adenovirus control, AAV-GFP or AAV-GFP-miR-1825, intraperitoneally. EdU was administered up to day 11, every other day to label proliferating cells (**Figure 5A** schematic). Hearts were harvested on day 12, miR-1825 transduced hearts showed a significant increase in heart/body weight ratio (**Figure 5B**). Immunohistochemistry was used to determine proliferating cells and miR-1825 transduced hearts showed a significant increase in EdU positive cells (**Figure 5C**), while WGA staining showed a significantly smaller cell size (**Figure 5D**), indicating newly formed cardiomyocytes. We also analyzed other tissues (liver and lungs) and found no significant difference in proliferating cells when compared to control (Supplementary Figure 11). These results indicate that miR-1825 can extend the proliferative window of neonatal mouse cardiomyocytes.

Direct injection of aav-mir-1825 improved heart function

To test the effect of miR-1825 on cardiac regeneration we performed LAD ligation in 22 week old adult, female mice, followed by intra-myocardial injection of either AAV-GFP (n = 9) or AAV-GFP-miR-1825 (n = 10) in the peri-infarcted region (Supplementary Figure 12). While infarction size and heart to body weight ratio, at the end of the study (day 28), showed a slight but not a significant decrease (Supplementary Figure 12), echocardiograph analysis showed slight improvement in fractional shortening (%FS) and ejection fraction (%EF), while cardiac output was significantly improved on day 14 but deteriorated by day 28 (Supplementary Figure 12). Moreover, miR-1825 transduced hearts showed less dilation at all time points as shown by diastole volume (vol. (d)), while a significant

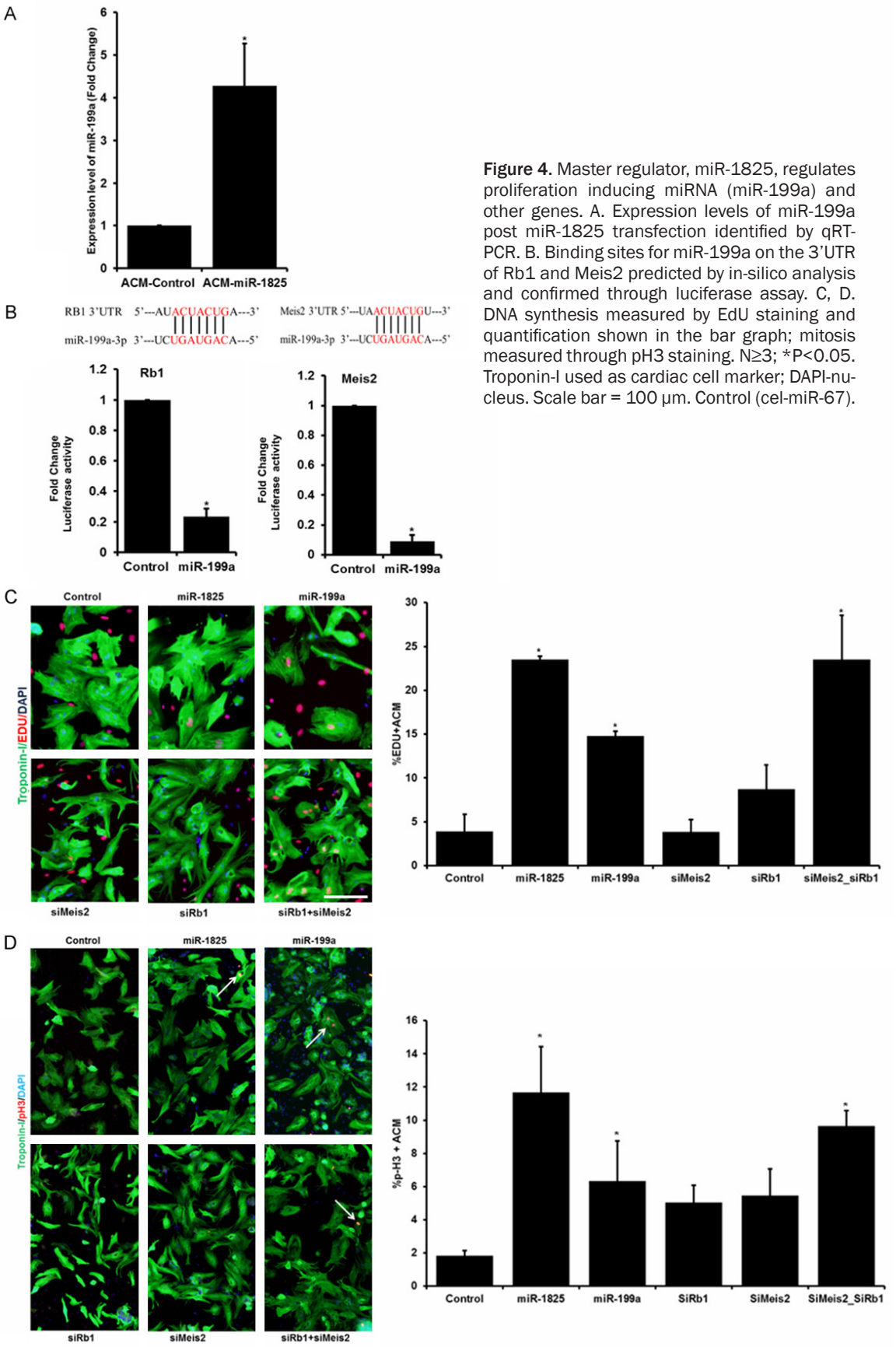

Figure 4. Master regulator, miR-1825, regulates proliferation inducing miRNA (miR-199a) and other genes. A. Expression levels of miR-199a post miR-1825 transfection identified by qRT-PCR. B. Binding sites for miR-199a on the 3'UTR of Rb1 and Meis2 predicted by in-silico analysis and confirmed through luciferase assay. C, D. DNA synthesis measured by EdU staining and quantification shown in the bar graph; mitosis measured through pH3 staining. N≥3; *P<0.05. Troponin-I used as cardiac cell marker; DAPI-nucleus. Scale bar = 100 μm. Control (cel-miR-67).

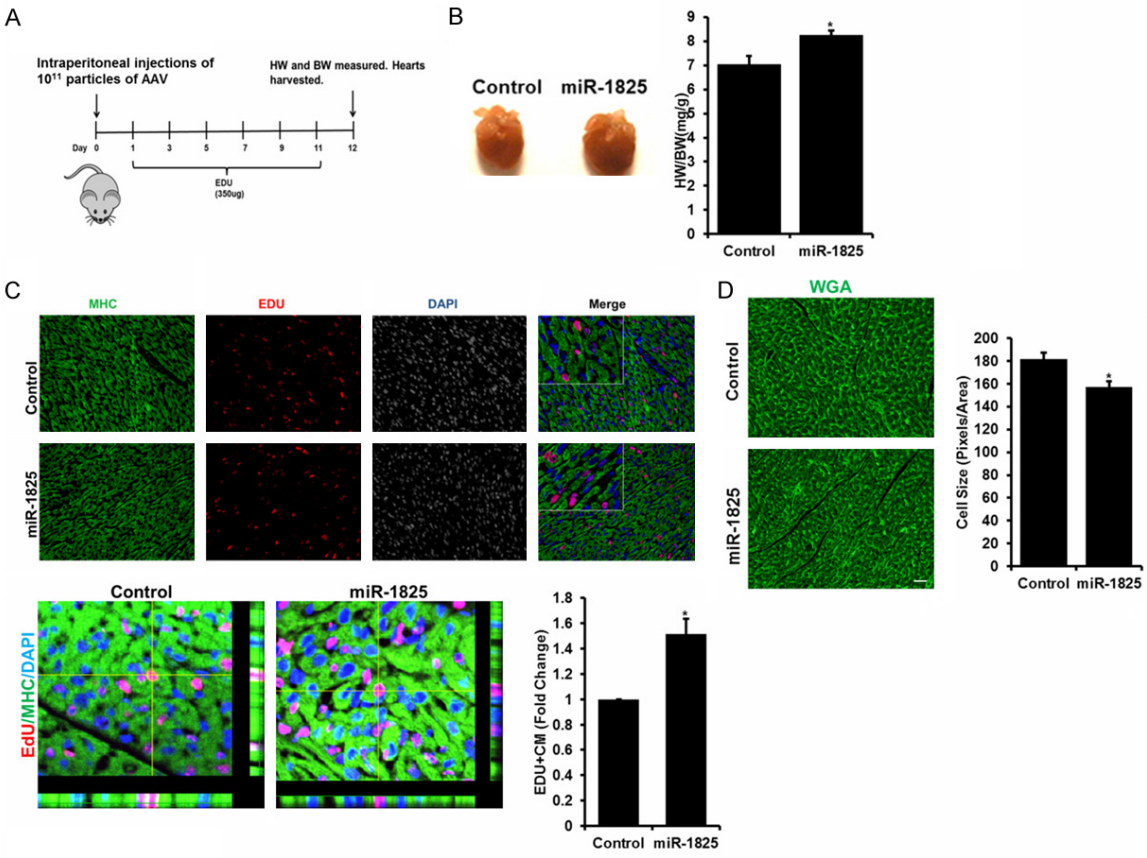

Figure 5. miR-1825 mediated proliferation results in increased cardiomyocyte number and heart size in neonatal mice. A. Schematic of adenoviral mediated control (AAV-GFP) and AAV-GFP-miR-1825 transduction in one day old neonatal mice. B. Heart size shown in picture on day 12 post injection; heart weight to body weight ratio shown in bar graph. C. Proliferating CMs identified through EDU; bar graph shows quantification of images. D. Cell size was measured using WGA staining; bar graph shows quantification of image size (30 cells per condition per trial; N = 3). *P<0.05. Myosin Heavy Chain (MHC) used as cardiac cell marker; DAPI-nucleus. N = 8. Scale bar = 1 mm.

improvement was observed only on day 14 (Supplementary Figure 12) but was not retained at day 28. Taken, together this data highlight the need for better delivery approaches in order to facilitate a prolonged and sustained delivery of miR-1825.

Hydrogel mediated prolonged delivery of mir-1825 improved heart function and induced cardiac regeneration post MI in adult mice

Due to insufficient regeneration observed through direct injection of AAV-miR-1825 in the peri-infarcted region, we developed a hydrogel mediated delivery method of AAV-miR-1825. We performed LAD ligation in 22 week old adult, female mice, followed by transduction of peri-infarcted region with 20 µL of Hydrogel + AAV-miR-1825 (n = 10) or hydrogel + AAV-GFP control (n = 6), with no treatment group (n = 4). We administered 350 µg EDU (intraperitoneally) every other day, up to day 12. Echocardiography was performed on day 7, 14, and 28 post-surgery and the hearts were harvested on day 30. We found a significant decrease in infarction size with hydrogel alone, while hydrogel + miR-1825 reduced the infarction size even further (and significantly lower than hydrogel alone) (**Figure 6A**). In addition, echocardiography analysis revealed a significant improvement in ejection fraction (%EF) and fractional shortening (%FS) on day 28. Moreover a measure of dilation, diastole volume (Vol (d)), while increased at a significant rate in the hydrogel group showed no significant increase in the miR-1825 group (**Figure 6B**). Indicating prevention of remodeling with miR-1825. Additionally, we looked at wall function through radial displacement and circumferential strain. MiR-1825 group showed a very significant improve-

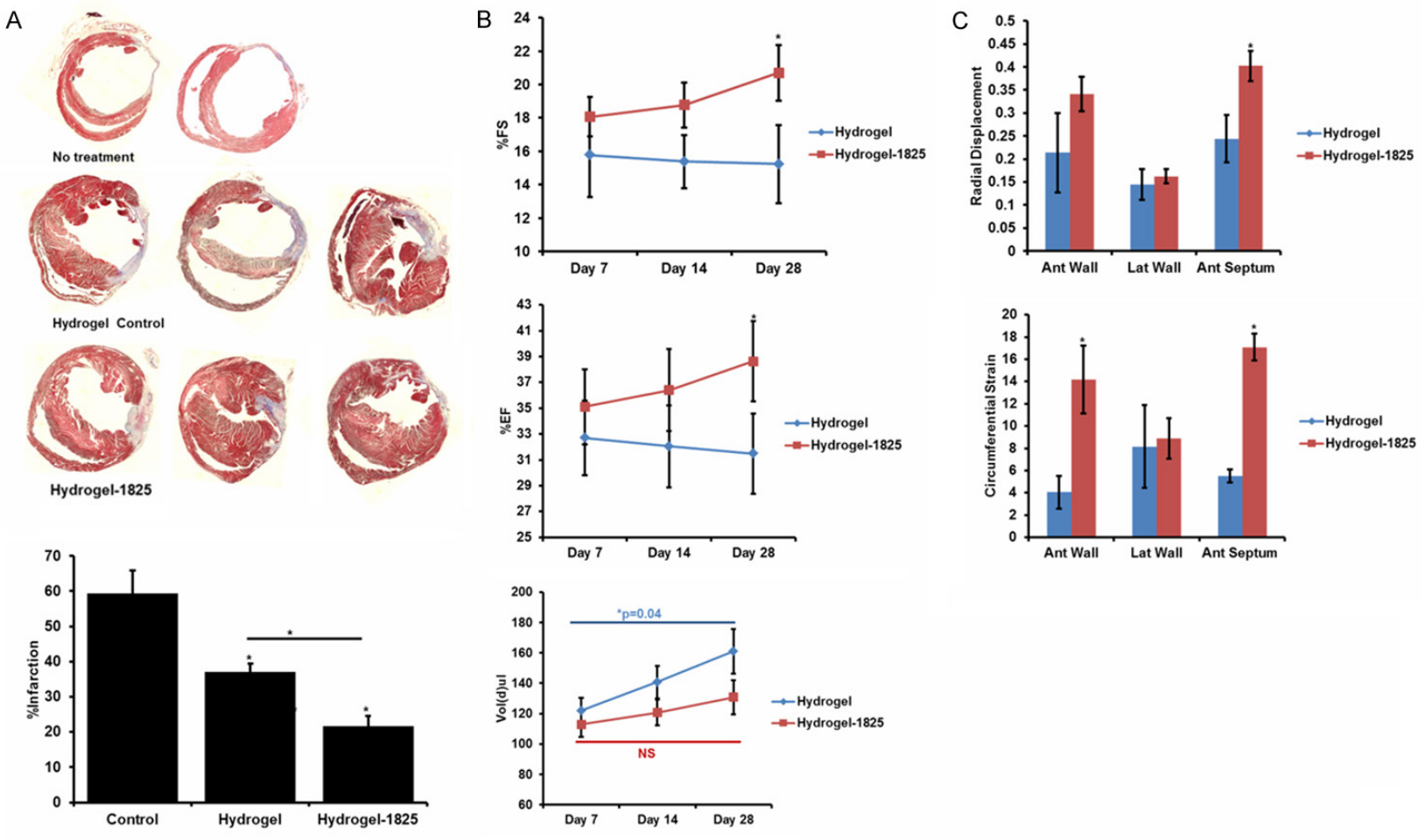
A
No treatment
Hydrogel Control
Hydrogel-1825
%Infarction
Control
Hydrogel
Hydrogel-1825
B
%FS
Day 7
Day 14
Day 28
Hydrogel
Hydrogel-1825
%EF
Vol(d)ul
*p=0.04
NS
C
Radial Displacement
Ant Wall
Lat Wall
Ant Septum
Circumferential Strain

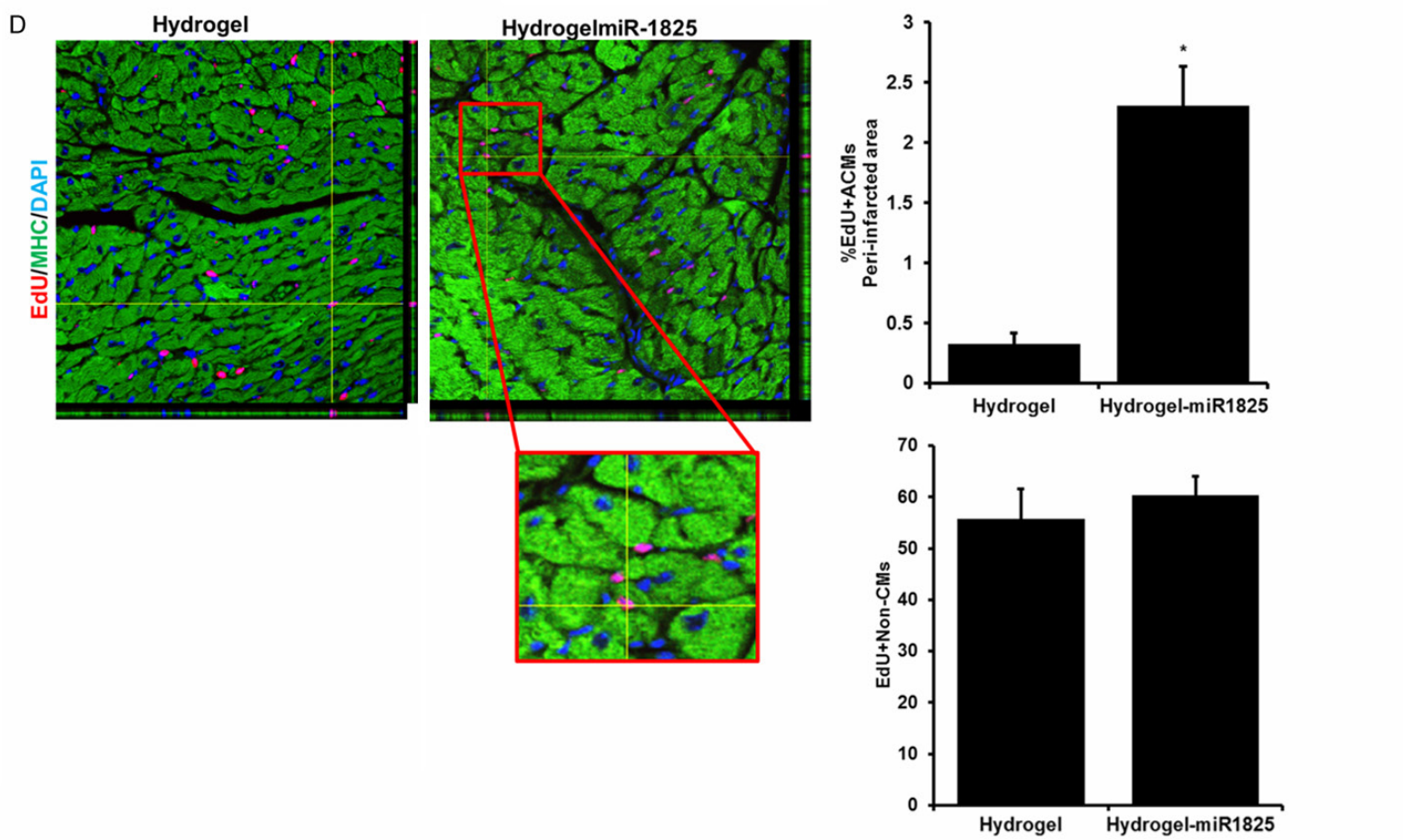

Figure 6. Hydrogel Mediated Prolonged Delivery of miR-1825 Improved Heart Function and Induced Cardiac Regeneration post LAD in Adult Mice. A. Infarction size 30 days post-surgery; bar graph shown quantification of infarction size. B. Percent fractional shortening (%FS), Ejection fraction (%EF), and diastole volume (measure for dilation) at day 7, 14, and 28 post-surgery. C. Measurement of wall function through radial displacement and circumferential strain. D. EDU positive CMs in the peri-infarcted region imaged using confocal microscope. EDU positive non-CMs were counted near the infarction site. *P<0.05. Myosin Heavy Chain (MHC) used as cardiac cell marker; DAPI-nucleus. N = 6 (Hydrogel), N = 10 (Hydrogel-1825).

ment in anterior wall and anterior septum function (**Figure 6C**), when compared to the hydrogel alone group.

Immunohistochemistry was performed to determine if miR-1825 induces proliferation of adult cardiomyocytes in-vivo in addition to preventing remodeling. Interestingly, 2.2% EdU positive cells were observed in the peri-infarcted region with miR-1825 (**Figure 6D**). All together hydrogel mediated miR-1825 delivery resulted in a significant increase in proliferation, reduction in infarct size and overall improvement in heart function following MI.

Discussion

We have previously identified microRNAs that promote proliferation of naturally quiescent adult cardiomyocytes. We have also shown a significant induction of DNA synthesis and mitosis with more than ten different microRNAs [34]. Here we demonstrate that one of these miRNAs, namely miR-1825, acts as a master regulator, regulating several genes and pathways involved in multiple cellular processes. In humans, miR-1825 is located in the 3'UTR region of the protein O-fucosyltransferases 1 (poFUT1) gene, upregulation of which has been shown to induce cell migration and proliferation [35, 36]. By in-silico analysis we did not find the presence of miR-1825 in mice and rats; however our results indicate that miR-1825 targets are conserved across species including mice, rats and humans.

Our in-vitro data using primary adult cardiomyocytes demonstrates that miR-1825 causes an increase in the total number of adult cardiomyocytes at each day post transfection, along with a significant increase in mono-nucleated (newly formed) cardiomyocytes. These results were also supported by an increase in cytokinesis as observed in adult cardiomyocytes transfected with miR-1825. This increase in cells number indicating an increased cell cycle activity was demonstrated with an increase in expression of CyclinD1 along with a decrease in cell cycle inhibitor, P16. These results establish miR-1825 as the key regulators of cell cycle genes promoting proliferation in otherwise non-dividing quiescent adult cardiomyocytes. To determine if miR-1825 mediated proliferative potential of adult cardiomyocyte changes with advanced age, we isolated adult cardiomyocytes from 17-month-old rats (~70 weeks) and transfected them with miR-1825. Interestingly, we found over 60% adult cardiomyocytes positive for DNA synthesis; 15 days post transfection (Supplementary Figure 13), indicating that miR-1825 can induce proliferation of adult cardiomyocytes even at later stages in life. This is analogous to inducing CM proliferation in a 50 year old human heart [37].

It has been recently shown that though stimulation of pre-existing cardiomyocytes complete cardiac regeneration can be achieved in neonatal mammals [38] and to some degree in adult mammals [8, 39]. Moreover, exogenous overexpression of transcription factors and growth factors have been shown to induce significant proliferation and regeneration in adult mouse hearts through induction of cardiomyocyte cell-cycle re-entry [40, 41]. Interestingly, microRNAs mediated proliferation has also been an emerging approach. Recent studies have shown miRNA (miR-204) to induce cardiomyocyte proliferation by regulating cell-cycle regulators (Jarid2, CyclinA2) [42, 43]. Additionally, a remarkable reduction in fibrosis, improvement in cardiac function and cardiomyocyte proliferation has been shown in adult mice through transient treatment with miRNAs post myocardial injury which can be attributed to cell proliferation, targeted by a specific miRNA (miR302-367) [44]. Following these studies we wanted to elucidate a mechanistic understanding of miR-1825 mediated proliferation observed in our adult rat cardiomyocyte system.

Our RNA-sequencing results identified genes regulated in multiple cellular pathways, of which the highest number was seen regulating mitochondrial function or metabolism. Our RNA sequencing data together with in-silico analysis identified NDUFA10 a mitochondrial gene to be a direct target of miR-1825. This was further confirmed by western blotting showing reduced NDUFA10 levels. NDUFA10 plays a direct role in mitochondrial function as was evident with fewer mitochondrial numbers following siRNA mediated knocked down of NDUFA10. While mutations in NDUFA10 has been shown to cause significant defects in oxidative phosphorylation and pathogenesis of hypertension [45] and Leigh disease [46], we show that direct inhibition of a mitochondrial gene NDUFA10 (observed with miR-1825) was key towards pro-

moting cell cycle re-entry. Moreover, miR-1825 inhibited ROS production, oxidative stress, and DNA damage in adult cardiomyocytes, in normal culture conditions as well as following exogenous oxidative stress (10 μM H_2O_2). This observation confirmed previous reports that quenching ROS promotes cell cycle re-entry and survival of cardiomyocytes [10, 47]. An acute reduction in the number of mitochondria can be helpful for cellular proliferation and maintenance, without hindering the cell's ability to generate energy for its survival. This has been shown previously by Canseco, et al. [48] where the reduction in number of mitochondria (due to a reduction in ventricular loading) in patients with left ventricular assist device led to an increase in proliferating cells through inhibition of DNA damage [48]. While others have shown the correlation between mitochondria and proliferation, we are the first to report a miRNA that causes a reduction in mitochondrial number, prevents DNA damage, and induces proliferation of adult cardiomyocytes. We also confirmed that with miR-1825, cells that were EdU positive showed reduced levels of mitochondrial gene VDAC (Supplementary Figure 14).

Here we identified that miR-1825 regulates multiple pathways, through direct inhibition (NDUFA10/mitochondrial function) and through upregulating miR-199a. Even though previous studies have shown miR-1825 to induce higher proliferation of adult cardiomyocytes when compared to miR-199a [9], we are the first to show miR-199 to be a downstream effector of miR-1825. In addition, this is one of the primary studies showing a mechanistic understanding of a robust multi-target miRNA, mediated induction of CM proliferation. Since proliferative capacity in a mouse heart is lost within a week post birth [49], we observed that intraperitoneal transduction with miR-1825 extended this proliferative window. Following miR-1825 transduction, day 12 mouse hearts, were bigger in size with smaller (newly divided) cells; indicating a significantly higher number of proliferating cells. Moreover, the cardiac specific nature of miR-1825 was confirmed with analysis of lung and liver tissue, which showed no difference in the rate of proliferating cells when compared to control. However, proliferation induction in adult mice, post ischemic injury would address the clinical relevance of miRNA as therapeutic. To address this concern we transduced 22 week old mouse hearts with miR-1825 post LAD ligation. Although, we observed a slight improvement in heart function along with reduced cardiac remodeling with miR-1825 on day 14, this improvement was not retained till day 28. This was evident with no significant reduction in infarction size on day 28. We acknowledged that intra-myocardial miRNA injection may not be an optimal delivery method for a prolonged delivery of miRNA; therefore we developed a hydrogel based delivery approach to increase the efficiency of transduction. As expected, hydrogel based delivery of miR-1825 showed a stupendous improvement in heart function (as measured through echocardiography) and prevented dilation and remodeling, when compared to the control hydrogel group. This may be attributed to the enhanced gene delivery efficiency and sustained expression of miR-1825 in the hydrogel group. In addition, together with a significant increase in proliferating cardiomyocytes in the peri-infarcted area the infarction size was also significantly reduced. We detected a prolonged expression of miR-1825 in the heart even after 30 days post hydrogel mediated delivery and our results indicate that hydrogel mediated miR-1825 delivery is a promising approach toward cardiac regeneration post injury.

This study holds a high translational potential due cardiomyocyte specific nature of miR-1825, longer shelf life, and ease of production and delivery. While reports suggest that 90% of stem cells transplanted in the heart are lost within the first few hours and in addition can raise concerns of tumor formation [50], some of these challenges can be addressed using therapeutic molecules to induce proliferation of endogenous cardiomyocytes. We believe this study is one of the first, to identify a multifunctional miRNA with robust effects towards cardiomyocyte proliferation, survival, and cardiac regeneration in-vivo. However, understanding how a single miRNA recruits other miRNAs and regulates multiple pathways is a subject for further research. Using downstream targets of miR-1825 having similar proliferative potential for in vivo delivery would prevent the concerns of off-target effects associated with miRNAs. The approach of inducing proliferation of endogenous cardiomyocytes has additional advantages of reducing the concerns of tumor forma-

tion, sometimes seen with fast dividing stem cells [50] when transplanted directly in the heart.

In conclusion, we understand the limitation with our in-vivo model, specifically, studying the transduction rate of AAV virus over the period of 30 days. However, unavailability of miR-1825 in mice and rats make this a challenging task. In the future we aim to determine this using GFP expression, which will also be present in AAV virus used. Additionally, a transgenic animal model with inducible miR-1825 expression in the heart would help study the effects of this miRNA during normal development and continuous administration post injury. Moreover, these results need to be further validated using larger animal models for cardiac regeneration along with the development of a minimally invasive hydrogel mediated miRNA delivery approaches, post MI.

Acknowledgements

This work is supported by National Institute of Health (NIH) grant 1R01HL-10690 to RPHA. The University Research Council (URC) Graduate Student Research Fellowship, University of Cincinnati to RP. Investigator grant provided by the Institutional Development Award (IDeA) from the National Institute of General Medical Sciences (NIGMS) of the NIH P20GM103638-04 to AP. We thank the department of Pathology and Laboratory Medicine at the University of Cincinnati College of medicine for their support. We thank Yamei Chen, Benjamin Weller, Jamie Fritz, Miso Rokvik, and Bereket Haile from the Habeebahmed Lab. AP acknowledges the University of Kansas New Faculty General Research Fund for support.

Disclosure of conflict of interest

None.

Authors' contribution

R.P and R.P.H.A designed and performed experiments, analyzed data, made the figures, and wrote the paper. S.V., M.N., M.J., J.C., S.D., performed experiments. J.B.B., A.P., and J.R. supervised experiments and edited the paper.

Abbreviations

ROS, Reactive Oxygen Species; NDUFA10, NADH Dehydrogenase (Ubiquinone) 1 Alpha Subcomplex; 10, 42 kDa; LAD, Left Anterior Descending Artery; EdU, 5-ethynyl-2'-deoxyuridine; pH3, phospho-Histone H3; HiPS-CMs, Human induced pluripotent derived cardiomyocytes; VDAC, Voltage dependent anion channel; Cel, Caenorhabditiselegans; ACMs, Adult cardiomyocytes.

Address correspondence to: Dr. Rafeeq PH Ahmed, Department of Pathology and Laboratory Medicine, College of Medicine, University of Cincinnati, 231 Albert Sabin Way, Cincinnati 45267, OH, USA. Tel: 513-558-4747; Fax: 513-584-3892; E-mail: Rafeeq.Habeebahmed@uc.edu

References

[1] Laslett LJ, Alagona P Jr, Clark BA 3rd, Drozda JP Jr, Saldivar F, Wilson SR, Poe C, Hart M. The worldwide environment of cardiovascular disease: prevalence, diagnosis, therapy, and policy issues: a report from the American college of cardiology. J Am Coll Cardiol 2012; 60 Suppl: S1-49.

[2] Heidenreich PA, Trogdon JG, Khavjou OA, Butler J, Dracup K, Ezekowitz MD, Finkelstein EA, Hong Y, Johnston SC, Khera A, Lloyd-Jones DM, Nelson SA, Nichol G, Orenstein D, Wilson PW, Woo YJ. Forecasting the future of cardiovascular disease in the United States: a policy statement from the American heart association. Circulation 2011; 123: 933-944.

[3] Murphy SL, Xu JQ, Kochanek KD. Deaths: final data for 2010. Natl Vital Stat Rep 2013; 61: 1-117.

[4] Go AS, Mozaffarian D, Roger VL, Benjamin EJ, Berry JD, Blaha MJ, Dai S, Ford ES, Fox CS, Franco S, Fullerton HJ, Gillespie C, Hailpern SM, Heit JA, Howard VJ, Huffman MD, Judd SE, Kissela BM, Kittner SJ, Lackland DT, Lichtman JH, Lisabeth LD, Mackey RH, Magid DJ, Marcus GM, Marelli A, Matchar DB, McGuire DK, Mohler ER III, Moy CS, Mussolino ME, Neumar RW, Nichol G, Pandey DK, Paynter NP, Reeves MJ, Sorlie PD, Stein J, Towfighi A, Turan TN, Virani SS, Wong ND, Woo D, Turner MB. Executive summary: heart disease and stroke statistics--2014 update: a report from the American heart association. Circulation 2014; 129: 399-410.

[5] Ahuja P, Sdek P, MacLellan WR. Cardiac myocyte cell cycle control in development, disease, and regeneration. Physiol Rev 2007; 87: 521-44.

[6] Bicknell KA, Coxon CH, Brooks G. Can the cardiomyocyte cell cycle be reprogrammed? J Mol Cell Cardiol 2007; 42: 706-21.

[7] van Amerongen MJ, Engel FB. Features of cardiomyocyte proliferation and its potential for

cardiac regeneration. J Cell Mol Med 2008; 12: 2233-44.
[8] Bergmann O, Bhardwaj RD, Bernard S, Zdunek S, Barnabé-Heider F, Walsh S, Zupicich J, Alkass K, Buchholz BA, Druid H, Jovinge S, Frisén J. Evidence for cardiomyocyte renewal in humans. Science 2009; 324: 98-102.
[9] Eulalio A, Mano M, Dal Ferro M, Zentilin L, Sinagra G, Zacchigna S, Giacca M. Functional screening identifies miRNAs inducing cardiac regeneration. Nature 2012; 492: 376-381.
[10] Kimura W, Xiao F, Canseco DC, Muralidhar S, Thet S, Zhang HM, Abderrahman Y, Chen R, Garcia JA, Shelton JM, Richardson JA, Ashour AM, Asaithamby A, Liang H, Xing C, Lu Z, Zhang CC, Sadek HA. Hypoxia fate mapping identifies cycling cardiomyocytes in the adult heart. Nature 2015; 523: 226-230.
[11] Puente BN, Kimura W, Muralidhar SA, Moon J, Amatruda JF, Phelps KL, Grinsfelder D, Rothermel BA, Chen R, Garcia JA, Santos CX, Thet S, Mori E, Kinter MT, Rindler PM, Zacchigna S, Mukherjee S, Chen DJ, Mahmoud AI, Giacca M, Rabinovitch PS, Aroumougame A, Shah AM, Szweda LI, Sadek HA. The oxygen-rich postnatal environment induces cardiomyocyte cell-cycle arrest through DNA damage response. Cell 2014; 157: 565-579.
[12] Ambros V. The functions of animal microRNAs. Nature 2004; 431: 350-355.
[13] Lee R, Feinbaum R, Ambros V. A short history of a short RNA. Cell 2004; 116 Suppl: S89-92.
[14] Lee RC, Feinbaum RL, Ambros V. The C. elegans heterochronic gene lin-4 encodes small RNAs with antisense complementarity to lin-14. Cell 1993; 75: 843-854.
[15] Yates LA, Norbury CJ, Gilbert RJ. The long and short of MicroRNA. Cell 2013; 153: 516-9.
[16] Seeger FH, Zeiher AM, Dimmeler S. MicroRNAs in stem cell function and regenerative therapy of the heart. Arterioscler Thromb Vasc Biol 2013; 33: 1739-46.
[17] Martinez-Sanchez A, Murphy CL. MicroRNA target identification-experimental approaches. Biology 2013; 2: 189-205.
[18] Yang JS, Lai EC. Alternative miRNA biogenesis pathways and the interpretation of core miRNA pathway mutants. Mol Cell 2011; 43: 915-926.
[19] Chiang HR, Schoenfeld LW, Ruby JG, Auyeung VC, Spies N, Baek D, Johnston WK, Russ C, Luo S, Babiarz JE, Blelloch R, Schroth GP, Nusbaum C, Bartel DP. Mammalian microRNAs: experimental evaluation of novel and previously annotated genes. Genes Dev 2010; 24: 992-1009.
[20] Cannell IG, Kong YW, Bushell M. How do microRNAs regulate gene expression? Biochem Soc Trans 2008; 36: 1224-31.
[21] Matkovich SJ, Hu Y, Dorn GW 2nd. Regulation of cardiac microRNAs by cardiac microRNAs. Circ Res 2013; 113: 62-71.
[22] Bell RM, Mocanu MM, Yellon DM. Retrograde heart perfusion: the langendorff technique of isolated heart perfusion. J Mol Cell Cardiol 2011; 50: 940-950.
[23] Xiao B, Sanders MJ, Carmena D, Bright NJ, Haire LF, Underwood E, Patel BR, Heath RB, Walker PA, Hallen S, Giordanetto F, Martin SR, Carling D, Gamblin SJ. Structural basis of AMPK regulation by small molecule activators. Nat Commun 2013; 4: 3017.
[24] Harris VM. Protein detection by simple western analysis. Methods Mol Biol 2015; 1312: 465-468.
[25] Paul A. Nanocomposite hydrogels: an emerging biomimetic platform for myocardial therapy and tissue engineering. Nanomedicine (Lond) 2015; 10: 1371-1374.
[26] Paul A, Manoharan V, Krafft D, Assmann A, Uquillas JA, Shin SR, Hasan A, Hussain MA, Memic A, Gaharwar AK, Khademhosseini A. Nanoengineered biomimetic hydrogels for guiding human stem cell osteogenesis in three dimensional microenvironments. J Mater Chem B Mater Biol Med 2016; 4: 3544-3554.
[27] Gaharwar AK, Avery RK, Assmann A, Paul A, McKinley GH, Khademhosseini A, Olsen BD. Shear-thinning nanocomposite hydrogels for the treatment of hemorrhage. ACS Nano 2014; 8: 9833-9842.
[28] Waters R, Pacelli S, Maloney R, Medhi I, Ahmed RP, Paul A. Stem cell secretome-rich nanoclay hydrogel: a dual action therapy for cardiovascular regeneration. Nanoscale 2016; 8: 7371-7376.
[29] Loeffen JL, Triepels RH, van den Heuvel LP, Schuelke M, Buskens CA, Smeets RJ, Trijbels JM, Smeitink JA. cDNA of eight nuclear encoded subunits of NADH: ubiquinone oxidoreductase: Human complex I cDNA characterization completed. Biochem Biophys Res Commun 1998; 253: 415-422.
[30] Shoshan-Barmatz V, Israelson A, Brdiczka D, Sheu SS. The voltage-dependent anion channel (VDAC): function in intracellular signalling, cell life and cell death. Curr Pharm Des 2006; 12: 2249-2270.
[31] Li Y, Park JS, Deng JH, Bai Y. Cytochrome c oxidase subunit IV is essential for assembly and respiratory function of the enzyme complex. J Bioenerg Biomembr 2006; 38: 283-291.
[32] Malliaras K, Terrovitis J. Cardiomyocyte proliferation vs progenitor cells in myocardial regeneration: the debate continues. Glob Cardiol Sci Pract 2013; 2013: 303-315.
[33] Mahmoud AI, Canseco D, Xiao F, Sadek HA. Cardiomyocyte cell cycle: meis-ing something? Cell Cycle 2014; 13: 1057-1058.

[34] Pandey R, Ahmed RP. MicroRNAs inducing proliferation of quiescent adult cardiomyocytes. Cardiovasc Regen Med 2015; 2.
[35] Liu S, Wang J, Qin HM, Yan XM, Yang XS, Liu C, Yang Q. LIF upregulates poFUT1 expression and promotes trophoblast cell migration and invasion at the fetal-maternal interface. Cell Death Dis 2014; 5: e1396.
[36] Annani-Akollor ME, Wang S, Fan J, Liu L, Padhiar AA, Zhang J. Downregulated protein O-fucosyltransferase 1 (Pofut1) expression exerts antiproliferative and antiadhesive effects on hepatocytes by inhibiting notch signalling. Biomed Pharmacother 2014; 68: 785-790.
[37] Sengupta P. The laboratory rat: relating its age with human's. Int J Prev Med 2013; 4: 624-630.
[38] Muralidhar SA, Mahmoud AI, Canseco D, Xiao F, Sadek HA. Harnessing the power of dividing cardiomyocytes. Glob Cardiol Sci Pract 2013; 2013: 212-221.
[39] Senyo SE, Steinhauser ML, Pizzimenti CL, Yang VK, Cai L, Wang M, Wu TD, Guerquin-Kern JL, Lechene CP, Lee RT. Mammalian heart renewal by pre-existing cardiomyocytes. Nature 2013; 493: 433-436.
[40] Rochais F, Sturny R, Chao CM, Mesbah K, Bennett M, Mohun TJ, Bellusci S, Kelly RG. FGF10 promotes regional foetal cardiomyocyte proliferation and adult cardiomyocyte cell-cycle re-entry. Cardiovasc Res 2014; 104: 432-442.
[41] Chakraborty S, Sengupta A, Yutzey KE. Tbx20 promotes cardiomyocyte proliferation and persistence of fetal characteristics in adult mouse hearts. J Mol Cell Cardiol 2013; 62: 203-213.
[42] Liang D, Li J, Wu Y, Zhen L, Li C, Qi M, Wang L, Deng F, Huang J, Lv F, Liu Y, Ma X, Yu Z, Zhang Y, Chen YH. miRNA-204 drives cardiomyocyte proliferation via targeting Jarid2. Int J Cardiol 2015; 201: 38-48.
[43] Cheng RK, Asai T, Tang H, Dashoush NH, Kara RJ, Costa KD, Naka Y, Wu EX, Wolgemuth DJ, Chaudhry HW. Cyclin A2 induces cardiac regeneration after myocardial infarction and prevents heart failure. Circ Res 2007; 100: 1741-1748.
[44] Tian Y, Liu Y, Wang T, Zhou N, Kong J, Chen L, Snitow M, Morley M, Li D, Petrenko N, Zhou S, Lu M, Gao E, Koch WJ, Stewart KM, Morrisey EE. A microRNA-hippo pathway that promotes cardiomyocyte proliferation and cardiac regeneration in mice. Sci Transl Med 2015; 7: 279ra38.
[45] Huang L, Jin X, Xia L, Wang X, Yu Y, Liu C, Shao D, Fang N, Meng C. Characterization of mitochondrial NADH dehydrogenase 1alpha subcomplex 10 variants in cardiac muscles from normal wistar rats and spontaneously hypertensive rats: implications in the pathogenesis of hypertension. Mol Med Rep 2016; 13: 961-966.
[46] Hoefs SJ, van Spronsen FJ, Lenssen EW, Nijtmans LG, Rodenburg RJ, Smeitink JA, van den Heuvel LP. NDUFA10 mutations cause complex I deficiency in a patient with Leigh disease. Eur J Hum Genet 2011; 19: 270-274.
[47] Puente BN, Kimura W, Muralidhar SA, Moon J, Amatruda JF, Phelps KL, Grinsfelder D, Rothermel BA, Chen R, Garcia JA, Santos CX, Thet S, Mori E, Kinter MT, Rindler PM, Zacchigna S, Mukherjee S, Chen DJ, Mahmoud AI, Giacca M, Rabinovitch PS, Aroumougame A, Shah AM, Szweda LI, Sadek HA. The oxygen-rich postnatal environment induces cardiomyocyte cell-cycle arrest through DNA damage response. Cell 2014; 157: 565-579.
[48] Canseco DC, Kimura W, Garg S, Mukherjee S, Bhattacharya S, Abdisalaam S, Das S, Asaithamby A, Mammen PP, Sadek HA. Human ventricular unloading induces cardiomyocyte proliferation. J Am Coll Cardiol 2015; 65: 892-900.
[49] D'Uva G, Aharonov A, Lauriola M, Kain D, Yahalom-Ronen Y, Carvalho S, Weisinger K, Bassat E, Rajchman D, Yifa O, Lysenko M, Konfino T, Hegesh J, Brenner O, Neeman M, Yarden Y, Leor J, Sarig R, Harvey RP, Tzahor E. ERBB2 triggers mammalian heart regeneration by promoting cardiomyocyte dedifferentiation and proliferation. Nat Cell Biol 2015; 17: 627-638.
[50] Jeong JO, Han JW, Kim JM, Cho HJ, Park C, Lee N, Kim DW, Yoon YS. Malignant tumor formation after transplantation of short-term cultured bone marrow mesenchymal stem cells in experimental myocardial infarction and diabetic neuropathy. Circ Res 2011; 108: 1340-1347.

Supplementary methods

Time-lapse videos

Adult Cardiomyocytes isolated from 8-12 weeks old rats and plated in 24 well-plates, transfected with either cel-miR-67 or miR-1825 were imaged for 20 hours with an image every 15 minutes. EVOS FL Auto Cell Imaging System (ThermoFisher Scientific) with an EVOS Onstage Incubator was used to keep cells in a regulated environment (37°C, 5% CO_2, Humidity). Bright field images were acquired at 20 × magnification.

Isolation of adult rat ventricular cardiomyocytes

Hearts were extracted from anesthetized rats and perfused using Krebs-Hanseleit bicarbonate (KHB) buffer. At time 10 min, 12.5 µl of 0.1 $CaCl_2$ was added to the circulation buffer solution. At time 15 min, 25 µl of 0.1 M $CaCl_2$ was added to make final concentration of 0.1 mM. Heart was then minced in KHB and filtered using a nylon mesh. Cells were then spun at ~300 rpm for 3 min at RT. Next, cells were re-suspended in solution containing 10% bovine serum albumin (BSA; sigma) in 1:1 ratio with KHB. 0.1 M $CaCl_2$ was added at 5 min intervals (3 times; 50 µl, 75 µl, and 100 µl) to achieve a final concentration of 1 mM [1].

Cells were then separated by sedimentation and re-suspended in DMEM containing 5% FBS and 1% penicillin-streptomycin (P/S). Pre-plating the cells in non-laminin coated plates was used to remove fibroblast contamination. Finally, cells were plated on mouse-laminin (Life Technologies, CA) coated plates and cultured at 37°C in 5% CO_2 and humidified atmosphere.

Transfection efficiency

Adult Cardiomyocytes were transfected with fluorescent labelled miRNA Dy547-cel-miR-67 using standard transfection protocol. Cells were imaged each day post transfection to check for RFP positive cells. Cytotoxic siRNA against Ubiquitin-C (UbC) siUbC was transfected using standard protocol and cells were fixed 4 days post transfection and stained for Troponin-I (Cardiomyocyte) and DAPI (nucleus). Control cells were transfected with cel-miR-67.

Immuno-staining

Cells were fixed with paraformaldehyde (4%) and incubated with primary antibodies overnight. Primary antibodies used included: rabbit mono-clonal antibody against Troponin-I (Santa Cruz Biotechnology sc-15368), histone H3 phosphorylation at serine 10 (Cell Signaling 9706S), Aurora B kinase (Abcam ab3609), VDAC (Cell Signaling 4661P), Nkx2.5 (Santa Cruz H114), and Anti-Oxoguanine 8 antibody (Abcam ab64548). Cells were then washed with PBS and incubated for 1 hour at RT with secondary antibodies conjugated to Alexa Fluor-488, -555, or -647 (Life Technologies). Click-IT EdU 555 and 647 imaging kit was used to identify EdU incorporation according to the manufacturer's instructions. DAPI was used to stain nuclei. Dihydrorhodamine 123 (Life Technologies, D-23806) was used to detect ROS by reconstituting in DMSO. Cells were incubated in 10 uM dihydrorhodamine 123 for 20 mins in the dark, followed by PBS wash. Wheat Germ Agglutinin (WGA), Alexa Fluor 488 conjugate (Invitrogen) was used to mark cell wall, as per manufacturer's protocol (Life Technologies, CA).

CM proliferation was measured by counting EdU (/pH3/ArB)$^+$ TnI$^+$ DAPI$^+$ CM per image. More than 3 images per condition, per trial (>1000 cells) were counted blindly by at least two individuals.

Cardiomyocyte cell count

Adult rat cardiomyocytes were transfected with either control cel-miR-67 or miR-1825 and each day post transfection a set of control and miR-1825 were fixed with 4% PFA, up until day 7. Fixed Cells were then permeabilized and stained with Tropinin-I (cardiac marker). Cardiomyocytes were counted for each set and fold change was calculated by normalizing the number of cells to its corresponding control (cel-miR-67 transfected) cells ($n \geq 3$).

Luciferase assay

3'UTR sequences used were as follows:

NDUFA10: >HmiT088389 3'UTR (binding sites in bold)

acgggccgccttctgctccagctgcatcacagtgatggccaagctgcatcagccgcactctcctggacgccatatagctttaagatc-
gggggagggtaaataatgcaaaaattgcacagtggaagaaggggtctcacaaaaagcaatccatcctgtagtataggtaatg-
gagttgggggaagcagcttccattctggatgtttggaacccttagctttgttttggaatggcccaccattct**cactgg**aaaacagtggtct-
gctgtgaaaggccagctctcggcagcccctgtggtttcagcgctgccgctctgtgtcattcaggttgtgcacattgtttttcttctgacttc-
cagaaataaaagtgtttccatgggaatttccccatcgtacgtctatgtgcgtgcgggcacgtcgaaactgcacacgtgcacacacgct-
gctctgggccctgtttggtgtggtgtggtttaattgaggcttacattatgctgaagagtttttctaaaggcctactgtatttatttagtaatgtgc-
tacattagagtagaaaaaataagaacgtgaagaagaaatagcaaaaggagaaaattaccacagatttacagaacaatatgtttta-
agagagacgttgagaaagattcacgtggccgtcctcagcgtctcaaactcctttgaagggagatttgagcttaggctgttgatgacataagat-
gcaaaagcaaaataatatactctctttattacccagaaaatcaagttgccagtcaaaactgagaaatgagaaagaaaatcagatttctt-
tattcatctctgttgaagcctagaaaaccaaaacaagctggttgtggttcagcatcatggtttaggaatcaagctgtcagttgtgagtcctact-
gaactgtgggttttccactgtaaagctccactgtgtccattaggaatcaggctgccagttgtgagtcctactgaactgtgggttttccactgta-
aagctccactgtgtccaatatggtagctcctagccacatgtgggtattgaaatttaaatgagctaaaatgtaatagagtttta-
aaattgggttccttggttg**cactgg**ccatagttcaggcactccacagccgcctgtgggcagtagttccagtgctggtgcagaggacgat-
gctctgctccccgcggaagctctaccaggcctcgctgctgcggagcatgcgaagaagatgcacactccttccctccttgcgtccgcctgccttt
tccctctccccttccttccctccttctttcctcctccttccctccctttccttttcttccttccatctgtccttgttttcctcccttcccttcctccctgcctcttt
ccttccctccttctcttccttccttccgtctgtccttgttttcctccctgcctctttccttccctccttctcttccttccttccttccgtctgtccttgttttcct-
cccttcccttcctccctgcctccttccttgttttaagaatttgaaaataaagtttcccaggagttttgaattggagtcgagatttaagtggct-
gaagttttgcatttcactaggaaaccaacagctttaatcatgaaatgaaagcacagctgggcattgggccagtcacagagtgtcttttgctct-
gagcacttcacaaacccattgtggaggggaggaaagaaaaagaaagccatctttaattatcttagctgttcctaatgtctttggctg-
caaagagctagctgtttccttcaaccttggtggttgcacgggtagtgtcctcagcagtgagagggcaggtctgccctgtggtcaggatt-
gcccttgtgaggggcagagctctccaaccatgcagggctccgtgtcggcatggtgtggactcgggtgctctgatcatcccctgtgtttgcgtct-
gaccctgtgtggttgcattcccttgatggagtgggaagtatgtaatttgtagtgctgaggacattcgtctgtttgattttctggtgttttcaat-
gacatgcatgttcagcagagaaagatgaataaacactgtccaattcttctctccacatagaagcctcaagaagaggtgaggagatgcccc-
gatttccttatttcagagcagtacatgcgttcgtctcacgaaagctcttacaactaaaacaacagcaccaacaaaccaggatcaaaataatc-
gtgcattttccaggattccatgttggacttctcagtgctttggagatcaggaaataatcatgctgttgcagcagtatggttttgtgtctggattt-
tattcatacaggcatgtgtttacaggcatgagaattctgtattgaaaagaaagtccttgtttttttctaacgtatctttctgttccatcaactgtta-
aaaccaaattgttaagaacattgagcttcttaggagagattacatgcagctacttaggaccacctcagcaaaatggagttgcctgggtag-
atagcagcagcagctcaccagccccacgctgccaggctgctggctgctgtccaccaggcagctgtggaacctccatgttctgcctaggtgtt-
gtggcaagaacagcagggaaacaggcggccgcctccaggccacaggtggacccagggaccttcagttacgccgcttcaattgaattcgtg-
gtggtttctctgctacagcagaagtggaagaagctcttgtcttgtttggcatttgtcccatttttttggctaataattggctttgaatttctctgt-
gccctgcttaccaattatagctttctggattggctgttcttagcagtgcaaatgtcaatgcaaagaagcaagcaggcggc-
tactttctgggaagaagcatagtccgtgctca**cactgga**tataaatctgcaagatttgggggtttggcaaaataggggtggagggaaagct-
gccatggctgtcagaaattggggcttttgaagaaaagcttgtgtaggcatcagc**cactggc**tggccagaattccatgaatggaagcaggt-
gcccgagtgatctggggctttacatgtggatataaatagaagccgggagcctgaggctttgctttaggaaaatcatgagccagaaaa-
cagaggaggtgattgtcagtagtcacctcacgccgctagtgttttctaatactctctcgaattgtcaaagcaaaggaccttataacagcaa-
cacgtgtgtgactcgaagcagcgagcttcccttgggaaaaggagcctcttctcagcagagggtcccagcctttctgtccttccccatcggaat-
gccaggctctgtgagtttggatgttggacattgccacctgaattccaggaggccggggagctccagtgatggacttgtccccaaaagagtg-
gtgctgttctcagagccataaatgttccactgaaagtgtctgtcccctggctcacgctggctgcgcttgcttgaaggaggctgatttaagggttc-
taataggaagacaaatgaaactgtcaaattttatctttaagcatgtgagtaagtttgctcattcgcttttactattgatgtatagttttaaaattct-
taatttaaaaattattttaatagtaaatttttcacaagtgaacacttttatctttaaattaaaattctgaagctccctagttagttagatccaatt-
gctggttacattttgggaagctctcattttagtgctatgtagtttcattgaataaacatgtttttaatgagaaaaaaaaaaaaaa

NDUFA10-mut: CS-HmiT088389-MT05-01 (with all 4 CACTGG sites deleted indicated above in bold).

Rb1: >HmiT016131-MT05 3'UTR (binding site in bold)

ggatctcaggaccttggtggacactgtgtacacctctggattcattgtctctcacagatgtgactgtataactttcccaggttctgtttatggcca-
catttaatatcttcagctctttttgtggatataaaatgtgcagatgcaattgtttgggtgattcctaagccacttgaaatgttagtcattgttatt-
tatacaagattgaaaatcttgtgtaaatcctgccatttaaaaagttgtagcagattgtttcctcttccaaagtaaaattgctgtgctttatg-
gatagtaagaatggccctagagtgggagtcctgataacccaggcctgtctgactactttgccttcttttgtagcatataggtgatgtttgctctt-

gtttttattaatttatatgtatattttttaatttaacatgaacacccttagaaaatgtgtcctatctatcttccaaatgcaatttgattgactgcccatt

caccaaaattatcctgaactcttctgcaaaaatggatattattagaaattagaaaaaaattactaattttacacattagattttattttactattggaatctgatatactgtgtgcttgttttataaaattttgcttttaattaaataaaagctggaagcaaagtataaccatatgatactatcat**actactg**aaacagatttcatacctcagaatgtaaaagaacttactgattattttcttcatccaacttatgtttttaaatgaggattattgatagtactcttggtttttataccattcagatcactgaatttataaagtacccatctagtacttgaaaaagtaaagtgttctgccagatcttaggtatagaggaccctaacacagtatatcccaagtgcactttctaatgtttctgggtcctgaagaattaagatacaaattaattttactccataaacagactgttaattataggagccttaattttttttcatagagatttgtctaattgcatctcaaaattattctgccctccttaatttgggaaggtttgtgttttctctggaatggtacatgtcttccatgtatcttttgaactggcaattgtctatttatcttttatttttttaagtcagtatggtctaacactggcatgttcaaagccacattatttctagtccaaaattacaagtaatcaagggtcattatgggttaggcattaatgtttctatctgattttgtgcaaaagcttcaaattaaaacagctgcattagaaaaagaggcgcttctcccctcccctacacctaaaggtgtatttaaactatcttgtgtgattaacttatttagagatgctgtaacttaaaataggggatatttaaggtagcttcagctagcttttaggaaaatcactttgtctaactcagaattatttttaaaaagaaatctggtcttgttagaaaacaaaattttattttgtgctcatttaagtttcaaacttactattttgacagttattttgataacaatgacactagaaaacttgactccatttcatcattgtttctgcatgaatatcatacaaatcagttagtttttaggtcaagggcttactatttctgggtcttttgctactaagttcacattagaattagtgccagaattttaggaacttcagagatcgtgtattgagatttcttaaataatgcttcagatattattgctttattgctttttttgtattggttaaaactgtacatttaaaattgctatgttactattttctacaattaatagtttgtctattttaaaataaattagttgttaagagtcttaa

Meis2: >HmiT011163-MT05 3'UTR (binding site in bold)

ccttcatcatgtaaagcaatcgcaaagcaagggggaagtttgcagagcatgccaggggactacgtttctcagggtggtcctatgggaatgagtatggcacagccaagttacactcctccccagatgaccccacaccctactcaattaagacatggacccccaatgcattcatatttgccaagccatccccaccacccagccatgatgatgcacggaggacccctacccaccctggaatgactatgtcagcacagagccccacaatgttaaattctgtagatcccaatgttggcggacaggttatggacattcatgcccaatagtataagggaactcaagggaaaaggaaacacacgcaaaaactattttaagactttctgaactttgaccagatgttgacacttaatatgaaattccagacagctgtgattatttttttacttttgtcatttttcatcaagcaacagaggaccaatgcaacaagaacacaaatgtgaaatcatgggctgactgagacaattctgtccatgtaaagatcctctggaaaaagactccgagagttata**actactg**tagtataaatataggaactaagttaaacttgtacatttctgttgatcacgccgttatgttgcctcaaatagttttagaagagaaaaaaaaatatatccttgttttccacactatgtgtgttgttcccaaaagaatgactgttttggttcatcagtgaattcaccatccaggagagactgtggtatatattttaaacctgttgggccaatgagaaaagaaccacactggagatcatgatgaacttttggctgaacctcatcactcgaactccagcttcaagaatgtgttttcatgcccggcctttgttcctccataaatgtgtcctttagtttcaaacagatctttatagttcgtgcttcataagccaattcttattattatttttgggggactcttcttcaaagagcttgccaatgaagatttaaagacagagcaggagcttcttccaggagttctgagccttggttgtggacaaaacaatcttaagttgggcagctttcctcaacacaaaaaaaaagttattaatggtcattgaaccataactaggactttatcagaaactcaaagcttgggggataaaaaggagcaagagaatactgtaacaaacttcgtacagagttcggtctattaattgtttcatgttagatattctatgtgtttacctcaattgaaaaaaaaaagaatgtttttgctagtatcagatctgctgtggaattggtattgtatgtccatgaattcttcttttctcagcacgtgttcctcactagaagaaaatgctgttacctttaagctttgtcaaatttacattaaaatacttgtatgaggactgtgacgttatgttaaaaaaaaaaaggtgttaagtcacaaaaagcggtaataaatatttcatttttgaaaaaaaaaaaaaaaaaaaaaaaaaaaaaaaaaa
aaaaaaaaaaaaaaaaaaaaaaaaaaaaa

Immuno-histochemsity

Animals were euthanized with an overdose of sodium pentobarbital and hearts were harvested on day 30 post surgery. Hearts were fixed in 4% paraformaldehyde (PFA) for 24 hours, followed by paraffin sectioning. Masson's trichrome and Hematoxylin and eosin (H&E) staining was performed. EdU and WGA staining were performed according to the manufacturer's instructions.

Human induced-pluripotent stem cell derived cardiomyocytes (HiPS)

HiPS-CMs were commercially purchased from Cellular Dynamics International (Wisconsin, USA) and cultured according to manufacturer's protocol. Cells were transfected according to the previously mentioned protocol and harvested on day 5 post transfection.

Western blot

Primary antibodies used: P16 (Cell Signaling ab51243), CyclinD1 (Cell Signaling 2922S), β-actin (Cell Signaling 4970S), Bcl-2 (Cell Signaling 2870S), NDUFA10 (Santa Cruz sc-107807), phospho-Rb (Cell Signaling 9308S), Meis1/2 (Santa Cruz sc-10599), COX-IV (Cell Signaling 4850).

RNA-sequencing analysis

Adult CMs transfected with cel-miR-67 or hsa-miR-1825 were used to isolate total RNA using Trizol (Invitrogen) according to the manufacturer's protocol. RNA was treated with DNase to remove contaminating DNA and cleaned with RNeasy kits (Qiagen). Sequencing was performed at Cincinnati Children's Hospital's DNA sequencing and Genotyping core using Illumina HiSeq2500. Single end 50 bp reads with 10 million reads were generated for each sample. Each library was mapped directly to the rat genome (version 6.0) allowing two mismatches per read and a 50% overlap with CLC Genomics (Qiagen). Each read was permitted to be mapped to 10 locations. Expression values were based on the number of unique reads mapped to each gene based upon the total number of reads mapped to the entire genome (TPM). Two different statistical tests (Kal's and Baggerly's Tests) were utilized which followed a false detection rate of $P<0.05$. Enrichment for specific gene ontology categories were examined using DAVID [2], g: Profiler [3], BiNGO [4], and PANTHER [5].

Primer sequences

NDUFA10:
F: TGAATTACACGACCGTCCCG
R: TCCACTTGTCACCCACATCG
COX-1:
F: ATCGCAATTCCTACAGGCGT
R: TGTTAGGCCCCCTACTGTGA
B-actin:
F: ACCCTAAGGCCAACCGTGAAA
R: GTACGACCAGAGGCATACAGG
GAPDH:
F: GCCAAAAGGGTCATCATCTCCG
R: ACATTGGGGGTAGGAACACGGA
MYH6:
F: TGATGACTCCGAGGAGCTTT
R: TGACACAGACCCTTGAGCAG
MYH7:
F: CCTCGCAATATCAAGGGAAA
R: CTACAGGTGCATCAGCTCCA
NKX2.5
F: ACCGCCCCTACATTTTATCC
R: GACAGGTACCGCTGTTGCTT

References

[1] Bell RM, Mocanu MM, Yellon DM. Retrograde heart perfusion: the langendorff technique of isolated heart perfusion. J Mol Cell Cardiol 2011; 50: 940-950.
[2] Huang da W, Sherman BT, Lempicki RA. Systematic and integrative analysis of large gene lists using DAVID bioinformatics resources. Nat Protoc 2009; 4: 44-57.
[3] Reimand J, Arak T, Vilo J. G: profiler--a web server for functional interpretation of gene lists (2011 update). Nucleic Acids Res 2011; 39: W307-15.
[4] Maere S, Heymans K, Kuiper M. BiNGO: a cytoscape plugin to assess overrepresentation of gene ontology categories in biological networks. Bioinformatics 2005; 21: 3448-3449.
[5] Mi H, Muruganujan A, Casagrande JT, Thomas PD. Large-scale gene function analysis with the PANTHER classification system. Nat Protoc 2013; 8: 1551-1566.

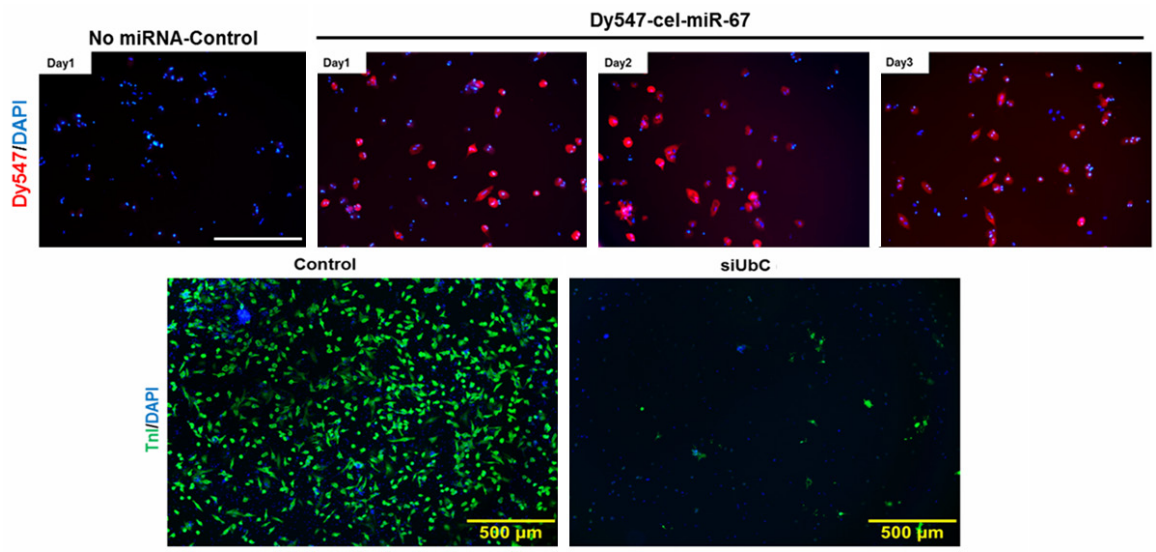

Supplementary Figure 1. Transfection efficiency of adult cardiomyocytes. Mock transfected (cel-miR-67) cardiomyocytes at day 1, Cardiomyocytes transfected with fluorescent labelled microRNA (Dy547-cel-miR-67) at day 1, 2, and 3 post transfection; Scale bar = 400 um. Cardiomyocytes transfected with control (cel-miR-67) and cytotoxic siUbC; Scale bar = 500 um.

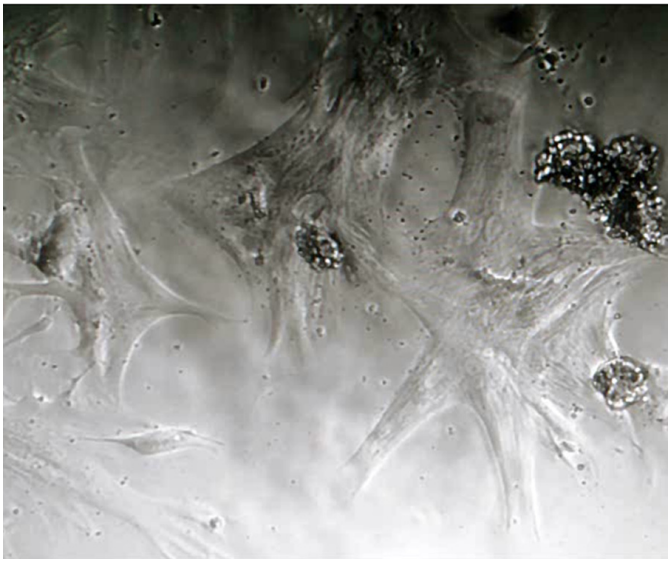

Supplementary Video 1. Video of adult cardiomyocytes 7 days post plating and transfection. Live cell imaging video; continuous video was recorded for 25 seconds showing beating cardiomyocytes.

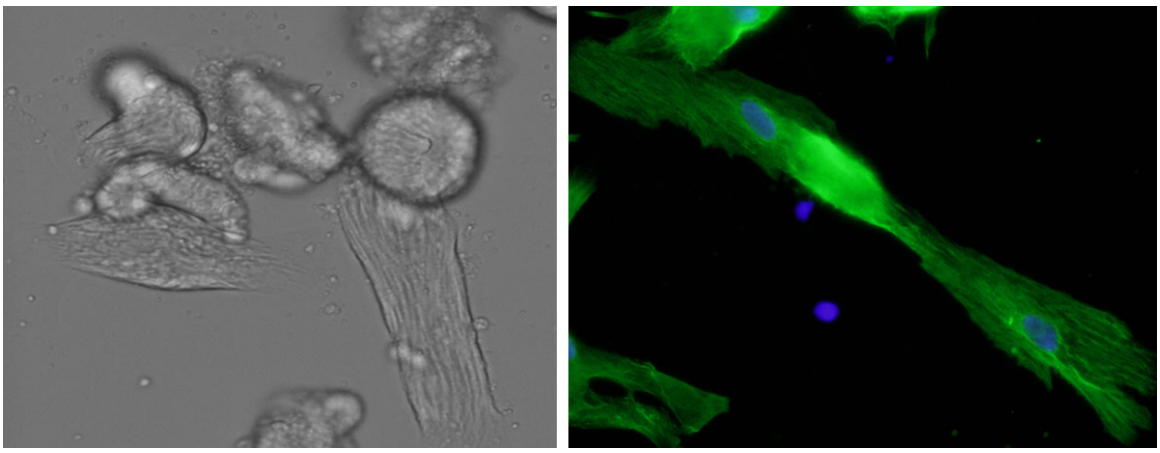

Supplementary Video 2. Video of proliferating adult cardiomyocytes transfected with miR-1825. Live cell imaging video; an image was taken at an interval of 15 minutes for 20 hours between day 3 and day 4. Color image shows a cardiac cell (green TnI) and its nucleus (Blue DAPI) at the end of the experiment.

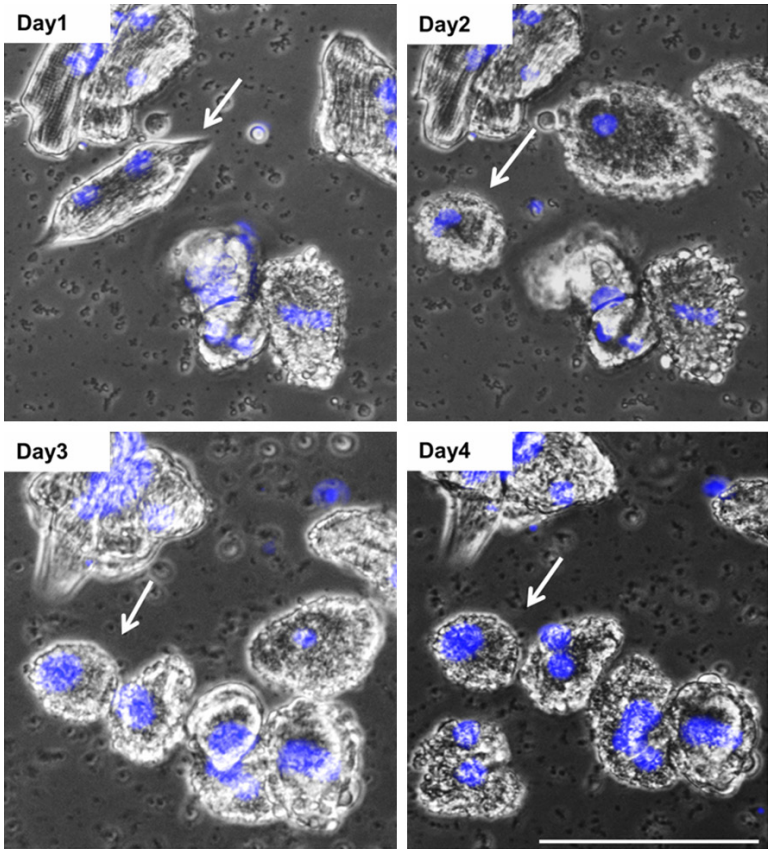

Supplementary Figure 2. Live cell imaging showed dividing cells. Individual cells were imaged everyday post transfection to capture dividing cardiomyocytes. White arrow shows a cardiomyocyte dividing into two between day 2 and day 3 post-transfection. DAPI (blue) denotes nucleus. Scale bar = 100 μm.

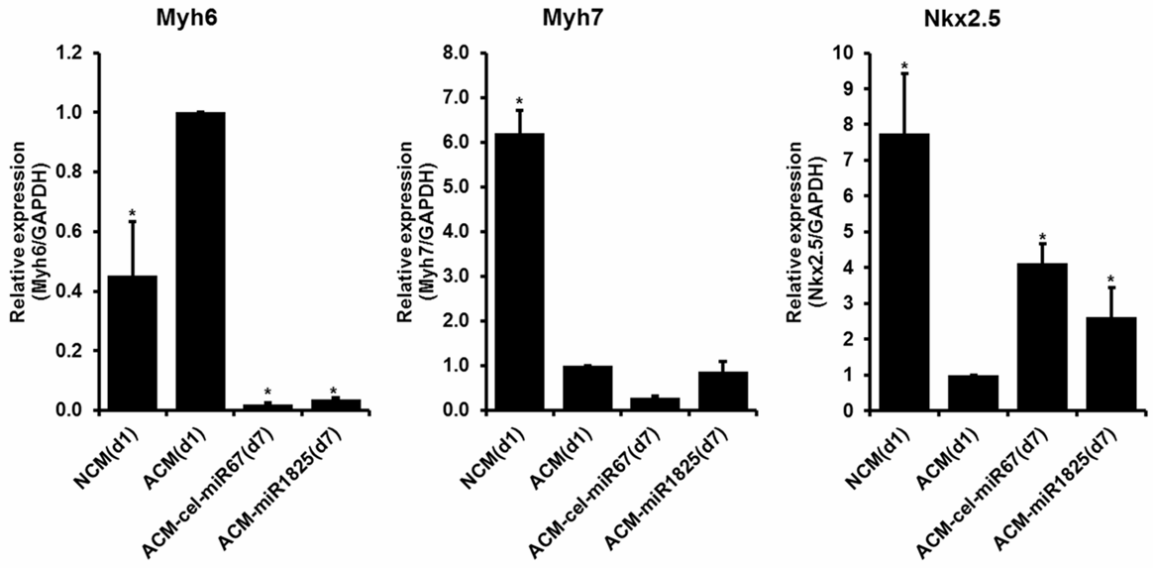

Supplementary Figure 3. Genes associated with cardiac differentiation are regulated in cultured adult cardiomyocytes. Myh6 (alpha MHC), Myh7 (beta MHC), and Nkx2.5 expression levels were measured using qRT-PCR. Fold change calculated after normalizing with GAPDH expression. N≥3, *P<0.05.

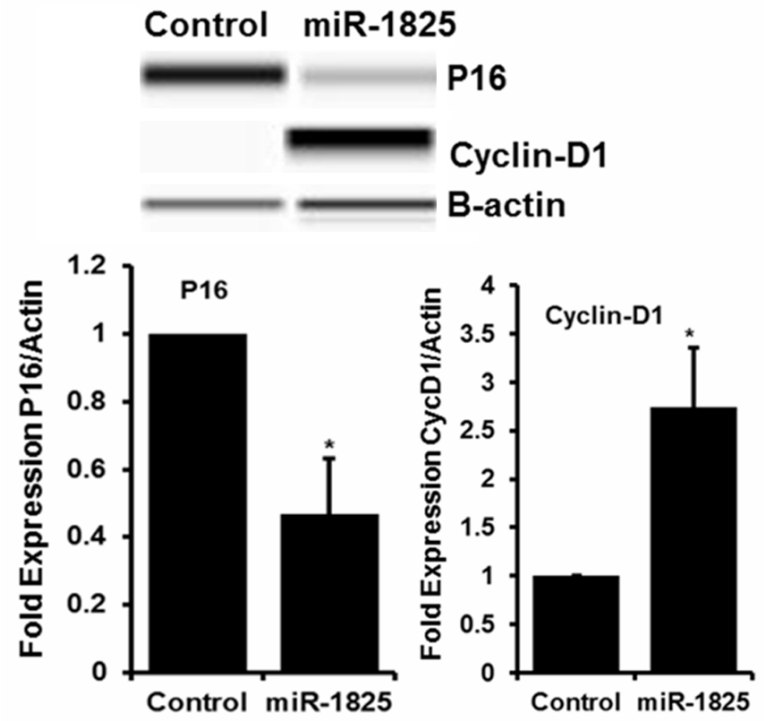

Supplementary Figure 4. Cell cycle genes are regulated by miR1825. Expression of P16 and CyclinD1 were measured by Wes Protein simple. Fold change calculated after normalizing with β-actin expression. N≥3, *P<0.05.

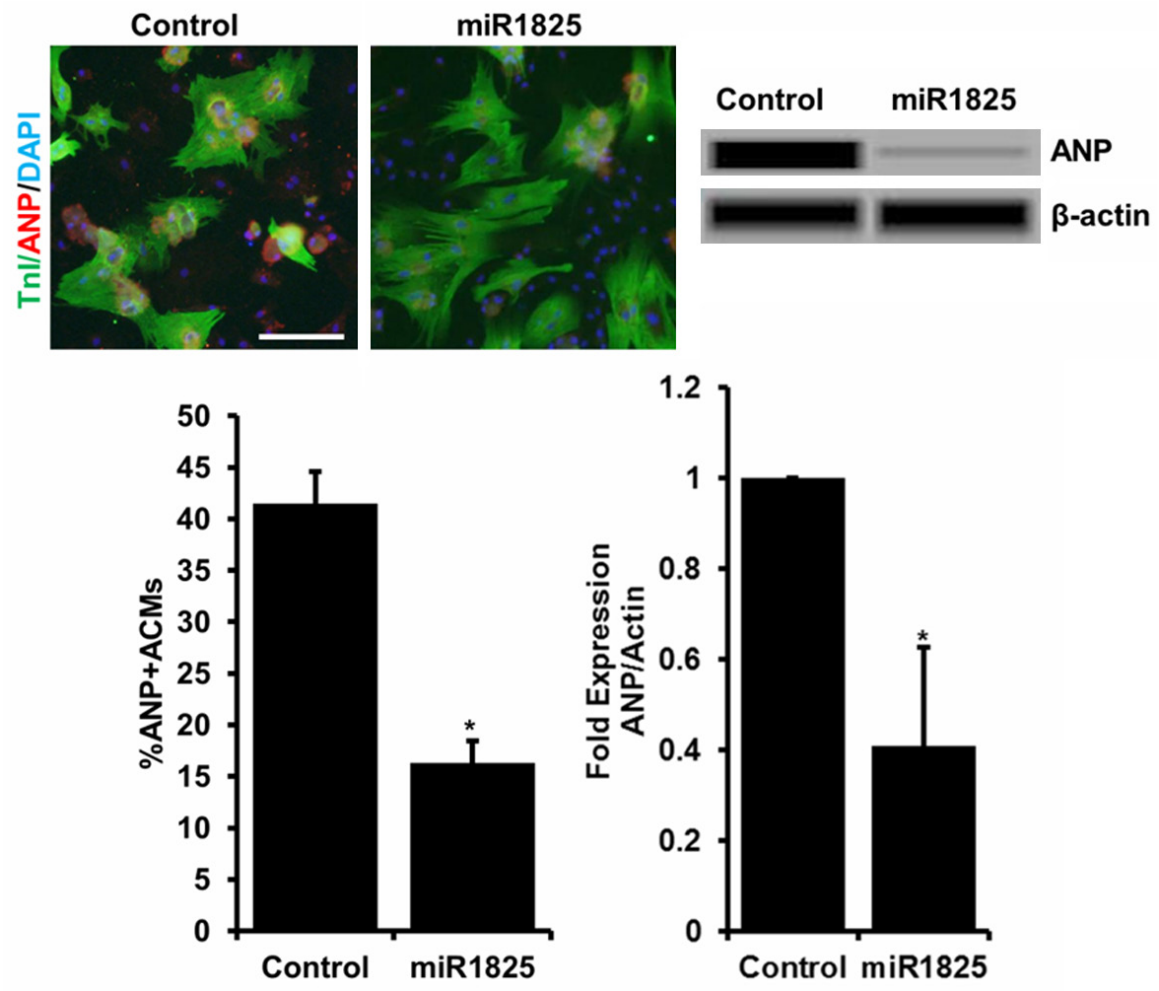

Supplementary Figure 5. miR-1825 prevents adult cardiomyocyte hypertrophy. Hypertrophy in ACMs was measured using ANP antibody (red). TnI (green; cardiac marker), DAPI (blue, nucleus). N = 3, *P<0.05. Scale bar = 5 mm.

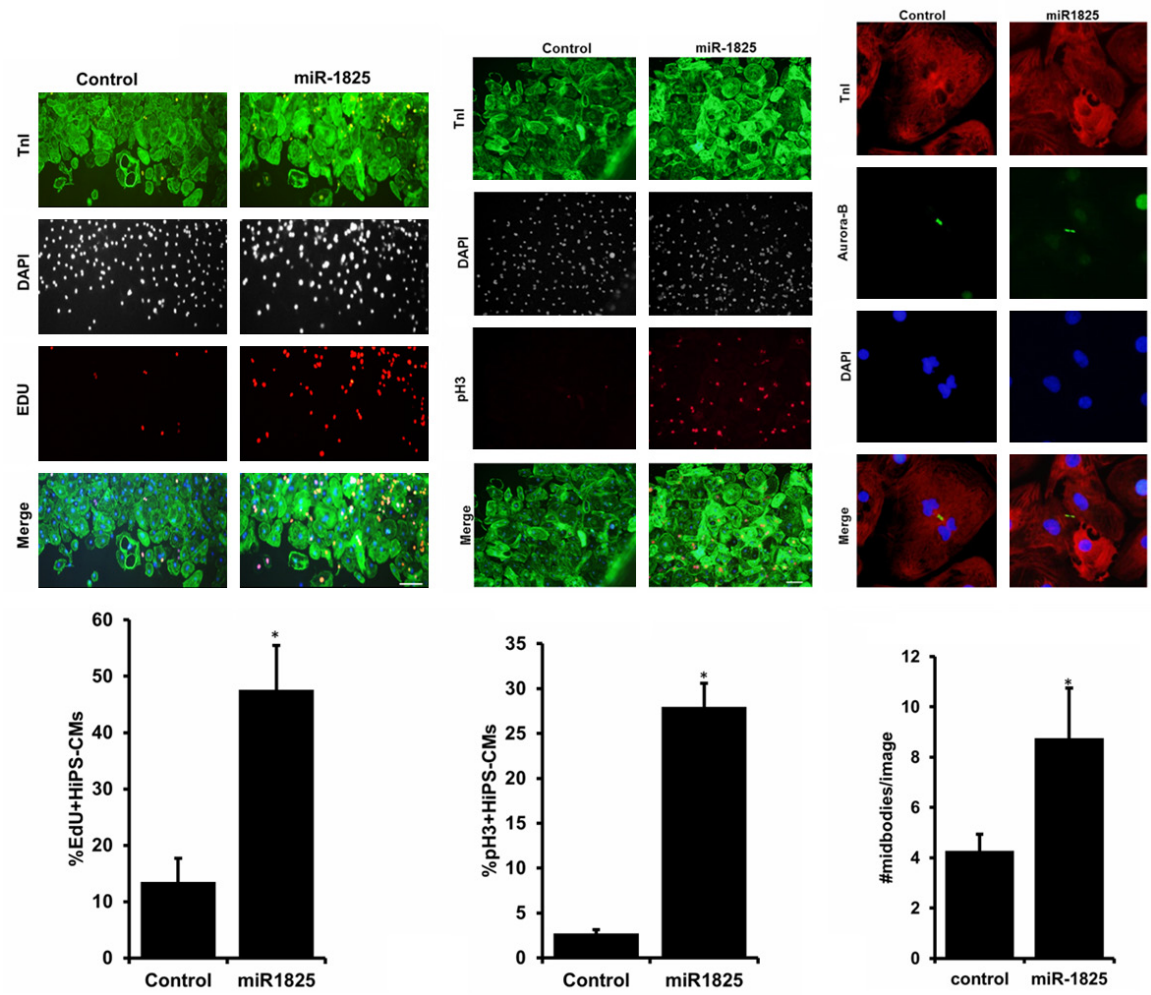

Supplementary Figure 6. miR-1825 induces proliferation of HiPS-CM. HiPS-CM proliferation was measured by EDU (DNA synthesis), pH3 (mitosis), and Aurora-B (mid-bodies). TnI (green; cardiac marker), DAPI (blue or white-pseudo color, nucleus). N = 3, *P<0.05. Scale bar = 200 μm.

miRNA	Fold
Mir190_1	-3.34
Mir183	-2.72
Mir26a	-1.4
Mir181b2	1.39
Mir181b1	1.56
rno-mir-199a	8.47
Mir199a	8.82

Genes	Fold
Ace3	3.59
Acta1	4.58
Actb_1	1.4
Actg2	1.56
Actn4	1.36
Aif1l	1.52
Ankh	1.26
AU018091	5.29
Axl	1.39
Casq1	3.77
Ccnb1	3.77
Ccnd1	1.76
Cd44	1.43
Cd82	1.56
Cdca3	2.95
Cdca8	3.03
Cdkn1a	1.5
Cercam	1.9
Ckap2	3.42
Cnn1	4.6
Col16a1	2.8
Col1a1	1.48
COL4A2	1.3
Col5a1	1.61
Csrp1	1.56
EFEMP2	1.47
Ehd2	1.52
Emp3	1.51
ENSRNOG00000014343	5.52
ENSRNOG00000029843	3.84
ENSRNOG00000031029	1.73
Fads3	1.42
Fam129b	1.29
Fam50a	3.33
Fen1	2.29
Fhl1	1.27
Fkbp10	1.49
Fkbp9	1.74
FTL1	1.59
G6pd	1.34
Gpx6	1.79
Gtse1	2.61
Hmga1	2.06
Hspb1	1.26

Htra1	1.9
Igsf1	3.23
Inha	3.07
Iqgap3	3.15
Itpr3	2.12
Kif20a	2.33
Kif22	2.44
Lrrc59	1.34
Ltbp2	1.27
Man1b1	1.34
Mcm3	1.8
Mcm5	2.6
Mmd	1.69
Mmp19	2.1
MT-ND2	1.82
Myl6	1.41
ND1	1.32
Nptxr	2.71
Olfml3	2.2
Pabpc1	1.18
Pcolce	1.15
PCOLCE2	2.42
Pdlim7	1.56
Phlda3	1.43
Pigu	2.05
Plk1	2.39
Pomp_2	1.67
Prc1	3.81
Ptgfrn	1.57
Ptgs1	2.19
Ptk7	1.44
Ptpla	1.75
Ptprn	2.53
PVR	1.57
RGD1561055	2.07
Rpl13_2	1.41
Rpn1	1.48
Rpn2	1.19
RRM2	2.79
Rrm2	3.1
Rtn3	1.39
S100a11	1.29
Sdc1	1.93
Sema7a	2.09
Sfrp4	4.33
Sh3bgrl3	1.59
Slc1a5	1.81
Snd1	1.3
Steap3	1.79
Stmn1_1	2.02
Sypl2	3.73
Tagln2	1.42
Tgfbi	1.37

Tgm2	1.8
Tkt	1.57
Ttyh3	1.73
Tuba1c	2.98
Tubb5	1.33
Tubb6	1.39
Ywhah	1.27
A430105I19Rik	-1.5
Acad9	-1.68
Acadl	-1.64
Acadm	-2.38
Acox1	-1.78
Acsf2	-1.71
Acss2	-1.43
Adam19	-1.85
Adcy5	-1.44
Afg3l2	-1.56
Ak3	-1.76
Akap1	-1.4
Aldoc	-3.43
Ampd3	-1.47
Anapc5	-1.29
Ankrd40	-1.4
Arpc5l	-1.5
Arvcf	-3.11
Atg13	-1.38
Atp1b1	-1.29
Atp5c1	-1.35
Atp5f1	-1.68
Atp6ap2	-3.4
Atp6v1e1	-1.42
B2m	-1.44
Bckdha	-2.02
Bnip3	-1.6
CACNA1G	-2.37
Calcoco1	-1.62
Cdh2	-2.53
Celf1	-1.43
Chchd3	-1.64
Clic4	-1.12
Cluh	-1.49
Cnp	-1.83
Coq9	-1.48
Cox15	-1.56
COX6A2	-1.75
Cox7b	-1.63
Cpe	-1.45
Cpt2	-1.48
Ctsc	-1.81
CYP51A1	-1.6
Ddc	-2.83
Dhrs4	-1.82
Dkk3	-1.65

Dlc1	-1.68
Dlst	-1.19
Dnaja3	-1.65
Dnpep	-1.46
Dynll2	-1.39
Ece1	-1.61
Echs1	-2.22
Eci1	-1.89
Efnb3	-2.8
Ehd4	-1.54
Eif3h	-1.45
ENSRNOG00000017202	-2.34
Fbln5	-2.06
Fdft1	-1.94
Fgf1	-1.79
Fndc1	-2.04
Foxo4	-1.86
Fuca1	-1.6
Fzd1	-1.49
Gadd45a	-1.62
Gbas	-1.54
Gcsh	-1.64
Ghitm	-1.66
Gja1	-1.3
Gja5	-2.96
Glis2	-1.61
Gpc1	-2.28
Grb14	-1.33
H3f3c	-1.34
Hadha	-1.27
Hadhb	-2.08
Hamp	-3.71
Herpud1	-1.43
Hes1	-1.63
Hibadh	-1.4
Hk1	-1.23
Hspb8	-1.22
Idh3B	-1.42
Idh3g	-1.38
Imp4	-1.61
Insig1	-1.65
Iscu	-1.35
Itfg3	-1.8
Itga11	-2.26
Itga9	-2.09
Ivd	-1.7
Kank1	-1.25
Kif1a	-3.36
Lmcd1	-1.4
Lrpap1	-2.34
Lrrc2	-2.36
Mafk	-1.39
Map1a	-1.34

Masp1	-2.9
Mavs	-1.52
Mccc2	-1.63
Mdk	-4.43
Mfap4	-2.43
Mical2	-1.29
Mrpl45	-1.82
Msmo1	-1.45
Mt2A	-3.11
Mtch2	-1.46
Mvp	-1.46
Mybpc3	-1.2
Myh14	-1.56
Ncam1	-1.75
Ncstn	-1.66
Ndufa10	-1.34
Ndufa5	-1.51
Ndufv2	-1.58
Nek9	-1.55
NFE2L1	-1.58
Nit1	-1.58
Nmt1	-1.7
Nrbp2	-1.88
Os9	-1.78
Panx2	-2.65
Paqr8	-2.05
Pbxip1	-1.6
Pcp4	-3.11
Pdhb	-1.43
Pgrmc2	-1.41
Phc2	-1.53
Phyh	-1.69
Pigk	-1.83
Pln	-1.72
Plxnb1	-1.4
Pmpcb	-1.59
Poldip2	-1.58
Ppap2b	-1.84
Ppm1a	-1.72
Ppp1r3c	-2.03
Ppp2r1a	-1.27
Prdx1	-1.44
Prdx3	-1.47
Prelp	-3.88
Prnp	-1.43
Prss23	-1.5
Ptpra	-1.51
R3hdm2	-1.44
Rbm20	-1.39
Rbm24	-1.53
Reg3b	-6.8
RGD1309492	-1.52
RGD735029	-1.77

Rps20_2	-1.25
Sardh	-1.54
Scn5a	-1.24
Scp2	-1.64
Sdf4	-1.34
Sdha	-1.93
Sdhd	-1.46
Sema5a	-1.83
Serpine1	-2.51
Setd3	-1.49
Sfrp1	-1.91
Shroom3	-1.44
Sidt2	-1.61
Skp1	-1.34
Slc12a7	-1.51
Slc16a1	-1.69
Slc25a23	-1.88
Slc25a3	-1.25
Slc25a30	-2.12
Slc41a1	-1.6
Smpd3	-3.45
Smpdl3a	-2.11
Sod2	-1.77
Sspn	-1.91
St3gal5	-2.1
Stat3	-1.48
Stradb	-2.81
Synpo2	-1.39
Tcp11l2	-1.72
Tep1	-1.35
Tfam	-1.81
Tmem182	-1.46
Tmem63b	-2.66
Tmem66	-1.54
Tmod1	-1.64
Tnnt2	-1.22
Tns1	-1.31
Tomm40	-2.09
Trnau1ap	-1.96
Tsc22d1	-1.73
Tspyl1	-1.57
Tubg1	-2.33
Txnl1	-1.49
Ube2b	-1.48
Ube2h	-1.43
Uqcrh	-1.31
Uqcrq	-2.75
Vamp1	-2.43
Vegfa	-1.36
Vegfb	-1.6
Vnn1	-2.21
Vrk3	-2.73
Znrf2	-1.76

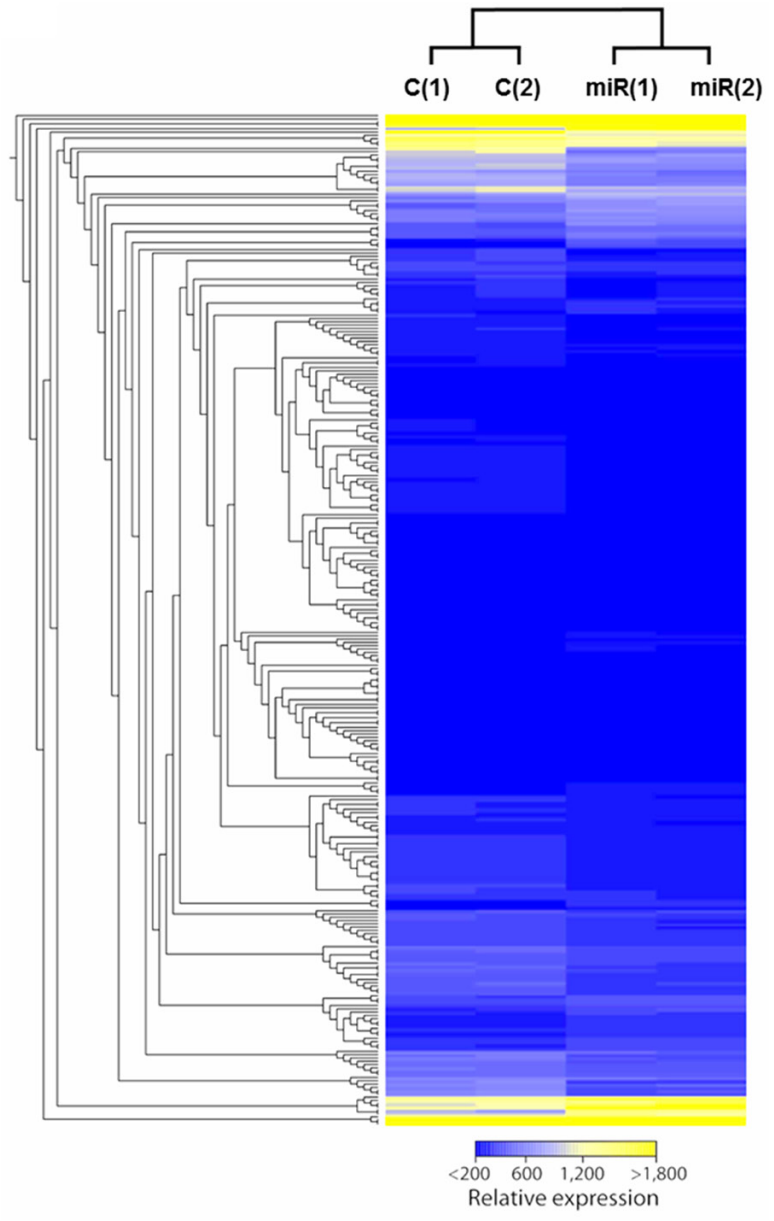
C(1)
C(2)
miR(1)
miR(2)
<200
600
1,200
>1,800
Relative expression

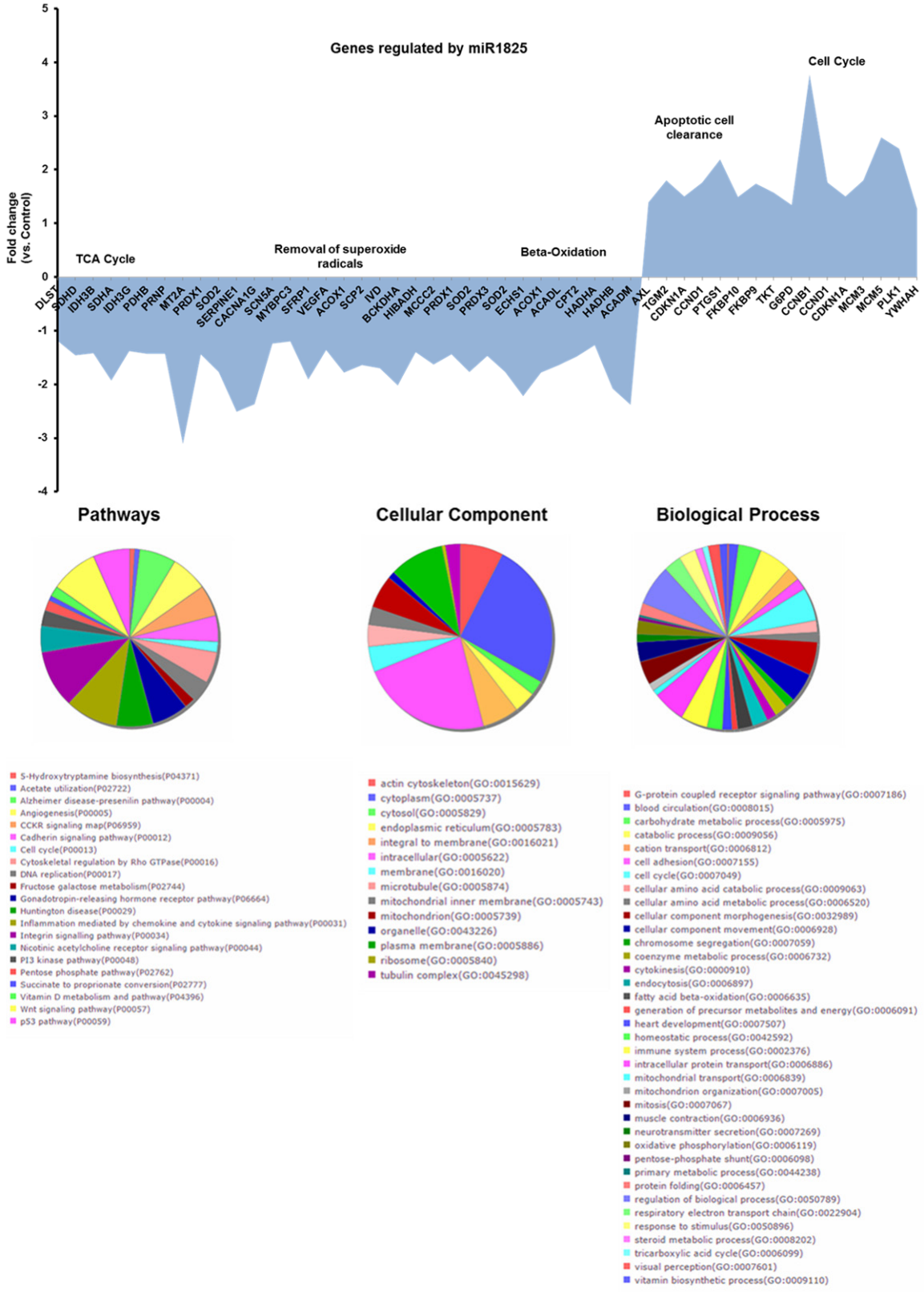

Supplementary Figure 7. Full list of genes and miRNAs regulated by miR-1825. Heatmap represents all the genes significantly regulated by miR-1825 (Relative expression represents TPM values). PANTHER analysis shows the pathways, cellular components, and biological processes regulated by miR-1825.

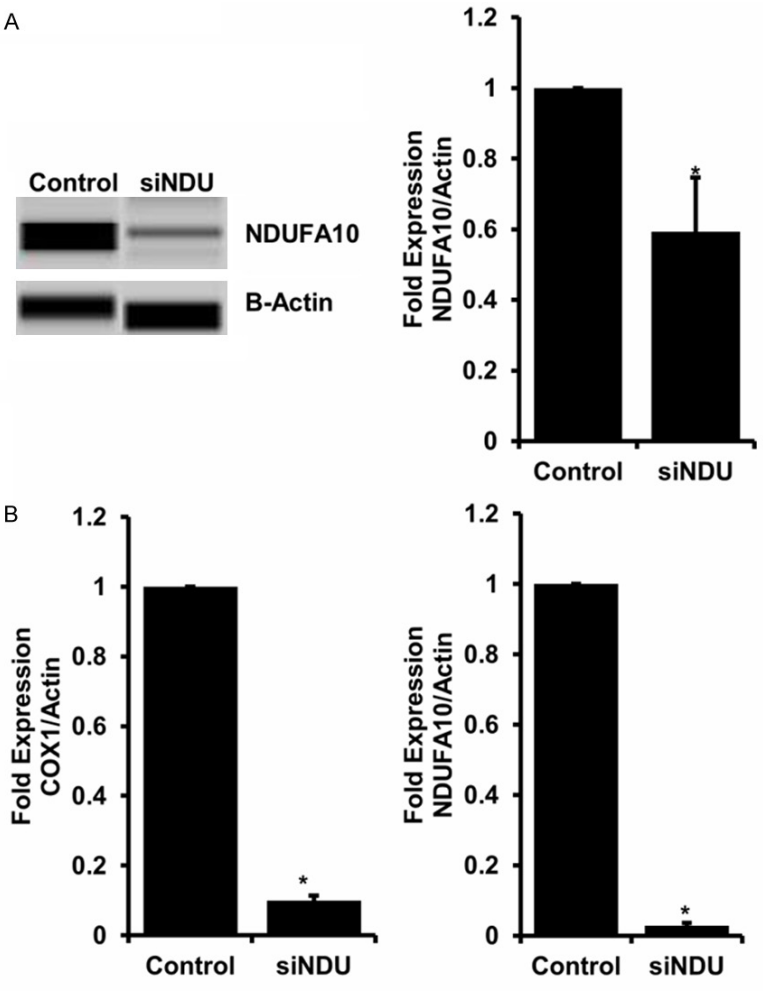

Supplementary Figure 8. siRNA mediated knockdown of NDUFA10 results in decrease in other mitochondrial genes. Efficiency of siNDUFA10 was measured at protein (A) and RNA (B) level, along with other mitochondrial gene COX1. Fold change calculated after normalizing with β-actin control. N = 3, *P<0.05.

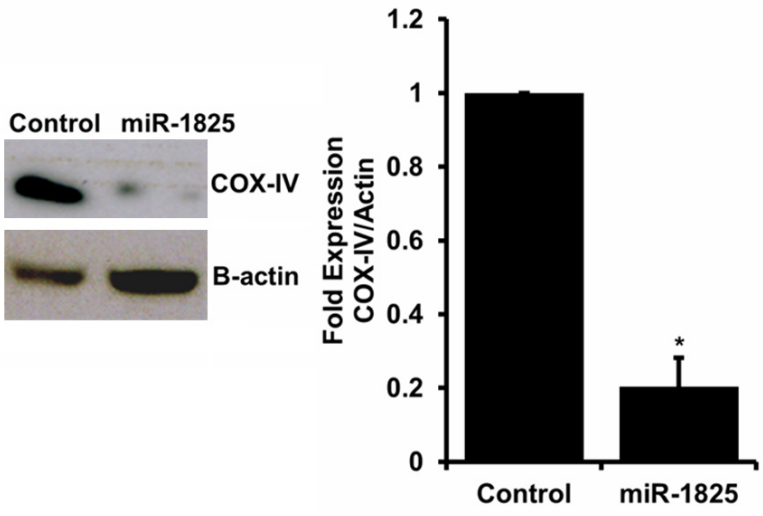

Supplementary Figure 9. miR-1825 causes reduction in COX-IV expression. COX-IV protein levels were used a marker for mitochondrial mass. Bar graph represents quantification of western blot images. Fold change calculated after normalizing with β-actin control. N = 3, *P<0.05.

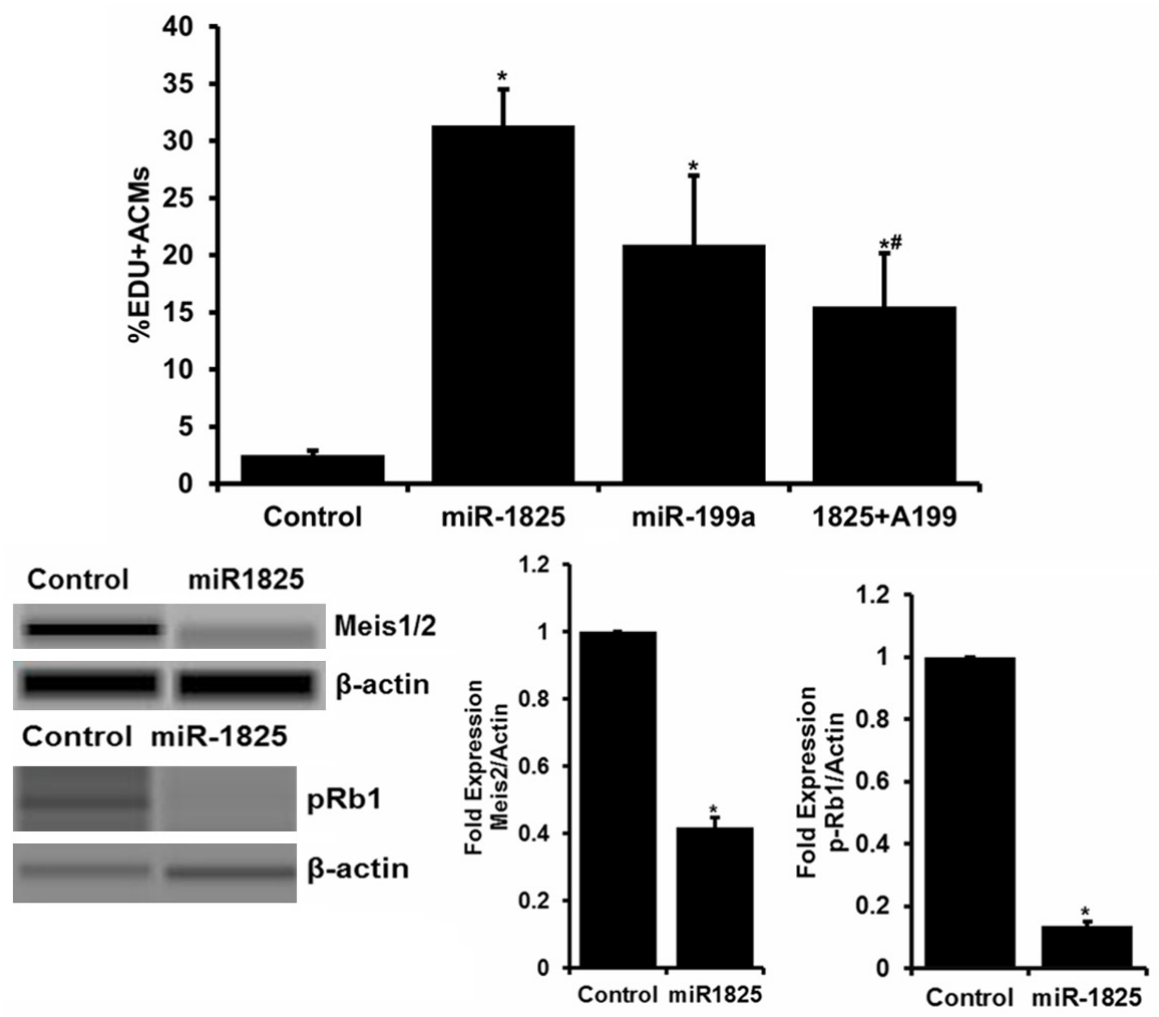

Supplementary Figure 10. miR-1825 works partly through miR-199a. EdU$^+$ cardiomyocytes were measured following transfection with Control miR-cel67, miR-1825, miR-199a, and miR-1825 together with inhibitor for miR-199a (A199) to determine relative contribution of each miRNA. N≥3; *P<0.05 (compared to control), #P<0.05 (compared to miR-1825).

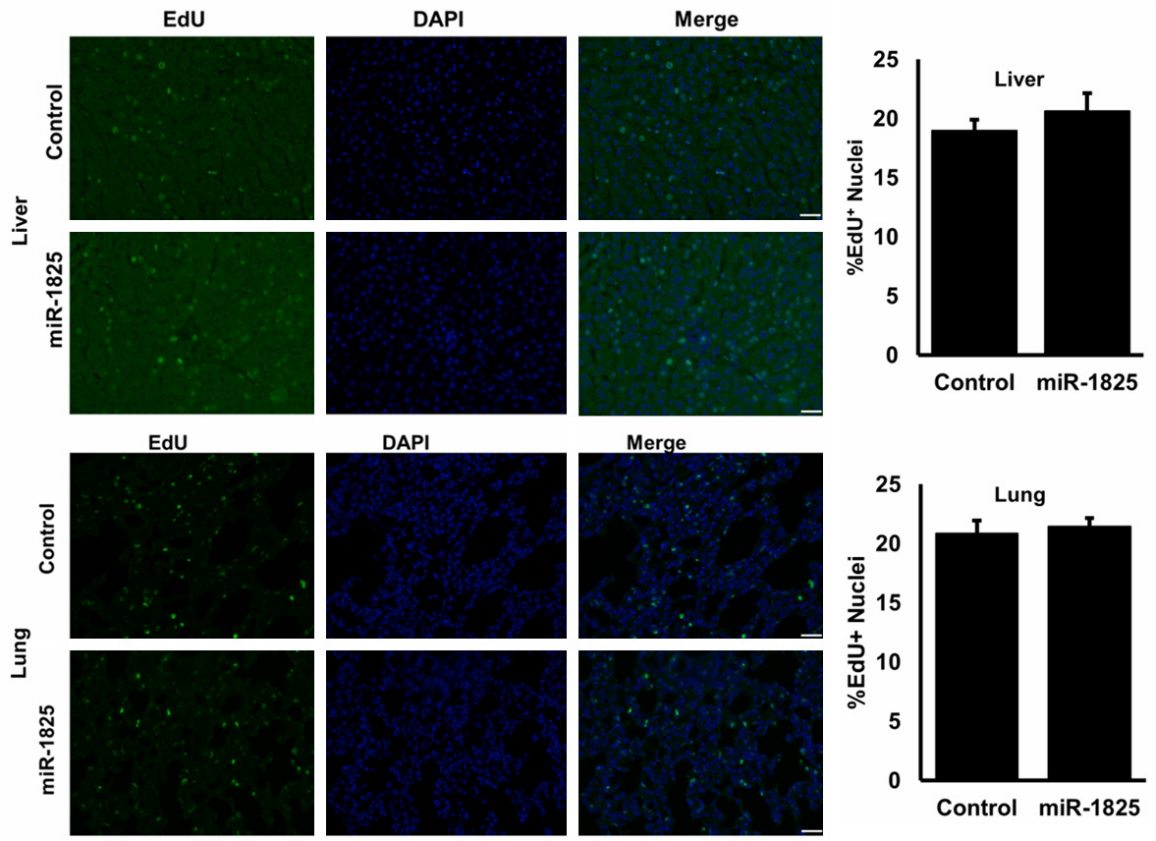

Supplementary Figure 11. miR-1825 has no effect on lung and liver cell proliferation. Proliferation measured in liver and lung tissue in neonatal (P1) rats transduced with miR-1825, intraperitoneally. EDU (green; DNA synthesis), DAPI (blue; nucleus). N = 3; NS = Not significant. Scale bar = 1 mm.

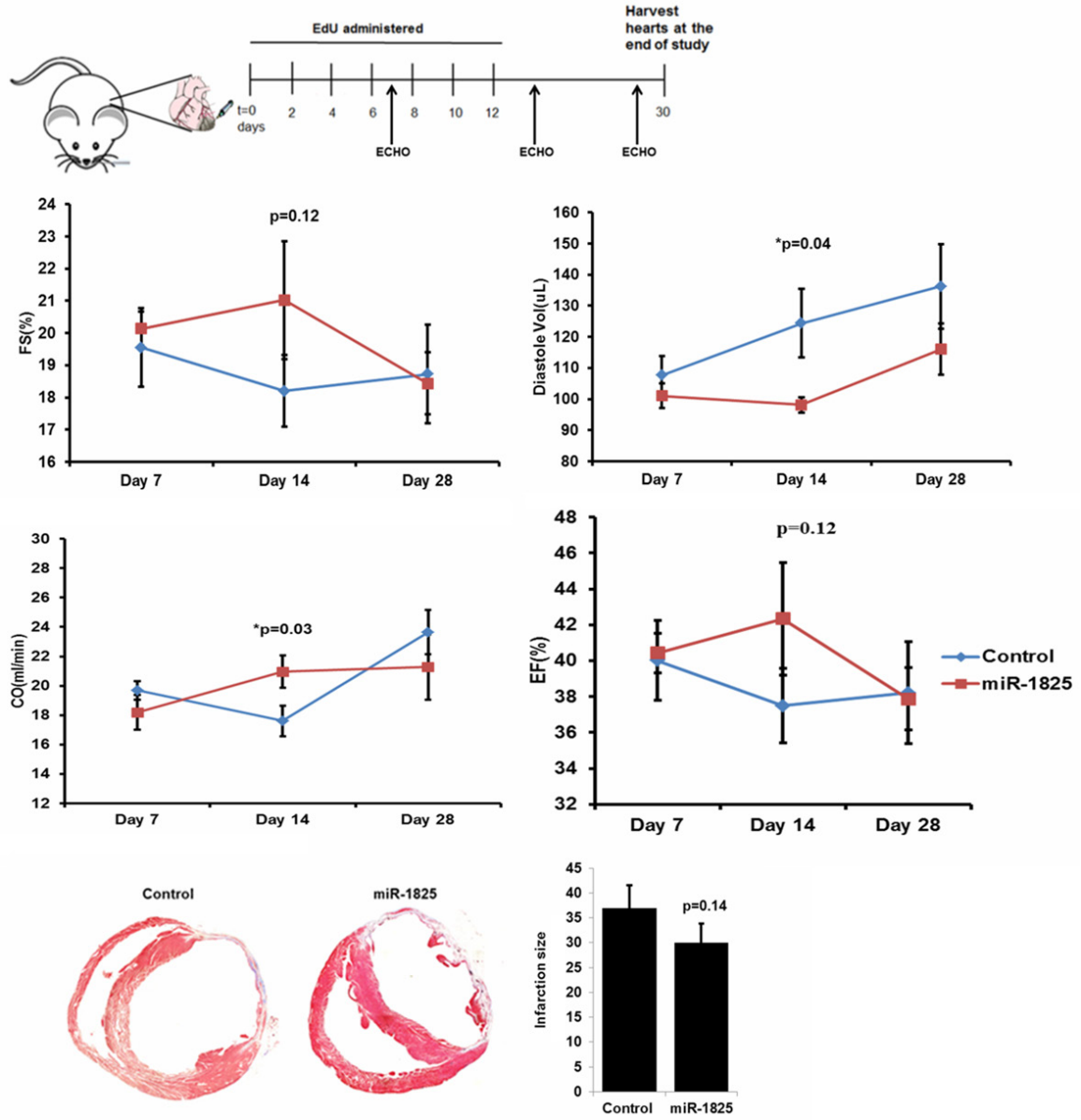

Supplementary Figure 12. Direct Injection of AAV-miR1825 does not show long-term effects. Schematic of experiment performed. Percent fractional shortening (%FS), percent ejection fraction (%EF), Cardiac Output (CO), and Diastole Volume as measured through echocardiography. Representative image for Infarction size and bar graph showing quantification of the data. N = 9 (control); N = 10 (miR-1825).

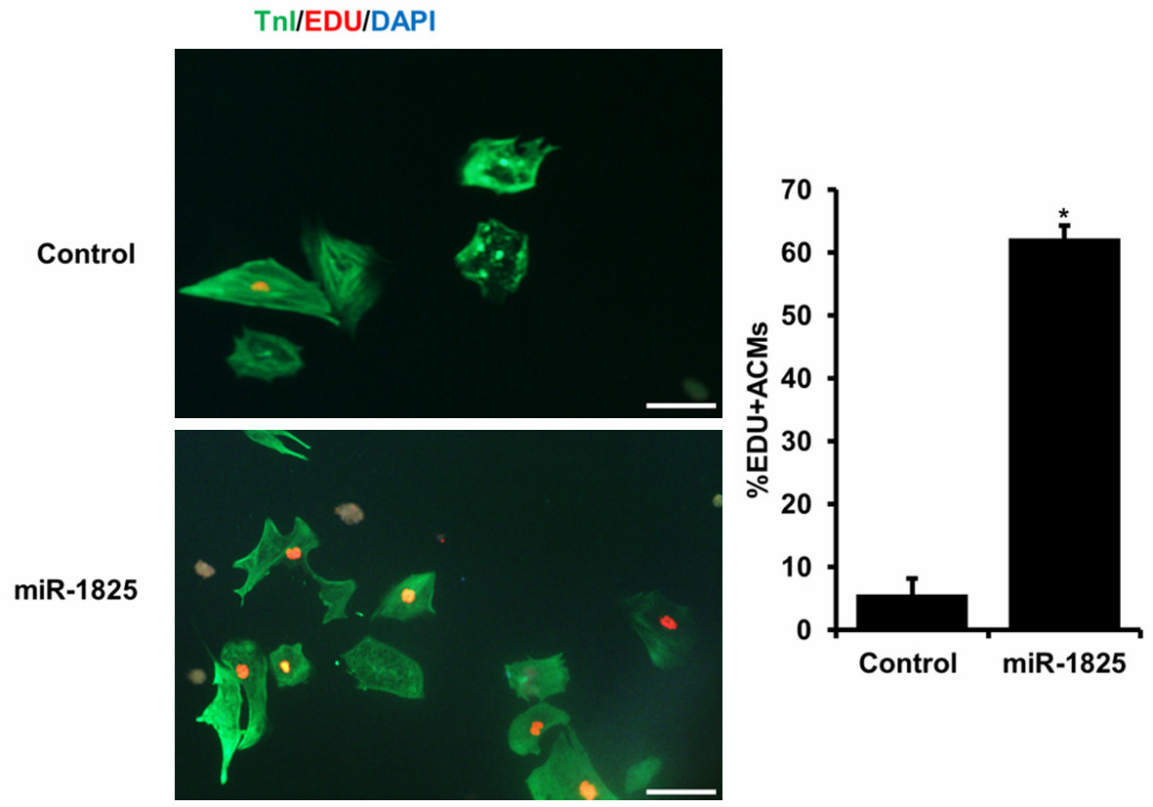

Supplementary Figure 13. miR-1825 also induces proliferation of adult cardiomyocytes from older rat heart. Adult cardiomyocytes from 17-month old rat were transfected with either control or miR-1825. EdU was used to measure DNA synthesis. *P<0.05; TnI (green) cardiac marker; DAPI (blue) for nucleus. Scale bar = 100 μm.

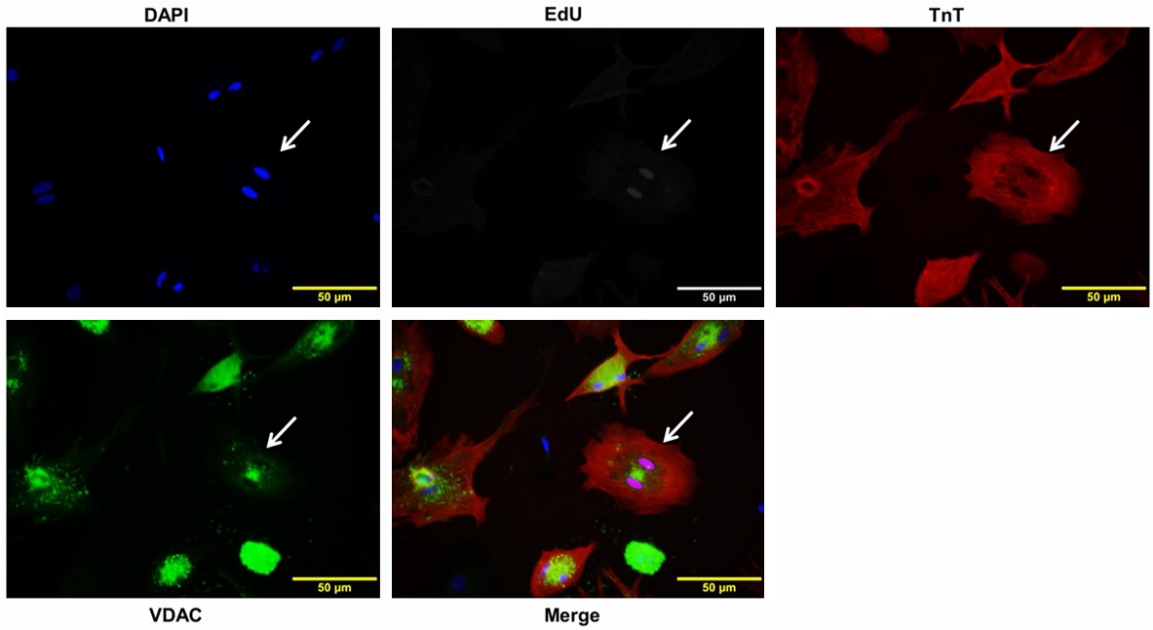

Supplementary Figure 14. Cardiomyocytes positive for EdU show reduced levels of VDAC compared to EdU negative cardiomyocytes. Adult Cardiomyocytes stained for VDAC (mitochondria), EdU, Troponin-T (TnT, cardiac marker), DAPI (nucleus). Scale bar = 50 μm.